The momentum dependence of the cross sections shown in Fig. 11 is clearly related to $\sigma(Kp)$ and $\sigma(Kn)$.

ACKNOWLEDGMENTS

This experiment was made possible in great part by the enthusiastic efforts of the High-Energy Physics Engineering staff and the Nimrod machine crews at the Rutherford Laboratory. We are indebted to R. Wimblett and the duty technicians for maintaining the liquid-hydrogen targets. A. Rush, R. MacKenzie, and H. R. Shaylor have given valuable technical assistance in preparing and running the experiment. We wish to thank Dr. G. F. Cox for the use of his program for calculating the effects of the Fermi motion. Two of us (A.A.C. and R.J.T.) wish to thank the Science Research Council for partial financial support.

PHYSICAL REVIEW VOLUME 168, NUMBER 5 25 APRIL 1968

Electron Trident and Pair Production at 500 MeV

B. GROSSETÊTE AND R. TCHAPOUTIAN
Ecole Normale Supérieure, Laboratoire de l'Accélérateur Linéaire, Orsay, France

AND

D. J. DRICKEY* AND D. YOUNT*
Stanford Linear Accelerator Center, Stanford University, Stanford, California

(Received 6 November 1967)

The cross sections, differential in the recoil positron energy, for trident and quartet production and for bremsstrahlung followed by pair and triplet production were measured for beryllium, aluminum, and platinum targets at a nominal incident electron energy of $E_0=500$ MeV and for recoil positron energies in the range above $0.80E_0$. The estimated experimental errors are about $\pm 6\%$ for the direct process and about $\pm 3\%$ for the double process at most points. The (pair+triplet) data for all three elements are in excellent agreement with theoretical predictions which contain detailed screening calculations and which take into account electron-electron bremsstrahlung and pair production in the electron field. A satisfactory fit (χ^2 probability 0.22) to the (trident+quartet) data was obtained with the no-screening calculations of Murota, Ueda, and Tanaka when the integration parameter (α in their notation) had a value 0.75 ± 0.05 and when quartets were taken into account by the substitution $Z^2 \rightarrow Z(Z+\eta)$, where η is the ratio of the total cross sections for electron-electron and electron-nucleon bremsstrahlung. If the timelike photon contributions, which amount to roughly 35% of the net cross section, are left out, the integration parameter has an optimum value of 2.00 ± 0.20. The corresponding χ^2 probability is much less than 0.01, indicating the necessity of the timelike terms.

I. INTRODUCTION

RECENTLY there has been considerable interest in pair production by electrons in the field of a nucleus, a process which may be useful in testing quantum electrodynamics at large momentum transfers.[1–6] Surprisingly, even the low-momentum-transfer region has not been studied with good precision. Furthermore, the differential cross section is quite complicated, and the available theoretical calculations contain large uncertainties except in a few cases[5,7] where detailed numerical integrations have been carried out.

The previous experiment most similar to our own was performed by Camac,[8] who determined the ratio of the direct (trident+quartet) cross section to the double cross section for bremsstrahlung followed by (pair+triplet) production.[9] His data, obtained on copper at an incident electron energy of $E_0=230$ MeV and at a final positron energy of $E=0.80E_0$, were believed to be accurate to about $\pm 25\%$. More recently, Bohm *et al.*[10] have measured the total trident cross section at 2.4 GeV to an estimated accuracy of $\pm 44\%$ in a propane bubble chamber.

The present experiment has grown out of the work of Browman, Grossetête, and Yount,[11] hereafter referred

* Supported by the U. S. Atomic Energy Commission.

[1] S. D. Drell, Ann. Phys. (N. Y.) 4, 75 (1958).
[2] J. D. Bjorken, S. D. Drell, and S. Frautschi, Phys. Rev. **112**, 1409 (1958).
[3] J. D. Bjorken and S. D. Drell, Phys. Rev. **114**, 1368 (1959).
[4] M. C. Chen, Phys. Rev. **127**, 1844 (1962).
[5] S. J. Brodsky and S. C. C. Ting, Phys. Rev. **145**, 1018 (1966).
[6] J. D. Bjorken and M. C. Chen, Phys. Rev. **154**, 1335 (1967); G. Reading Henry, *ibid.* **154**, 1534 (1967).
[7] E. G. Johnson, Jr., Phys. Rev. **140**, B1005 (1965).
[8] M. Camac, Phys. Rev. **88**, 745 (1952). A similar experiment was carried out at 31.5 MeV by L. Criegge, Z. Physik **158**, 433 (1960).
[9] "Tridents" and "quartets" refer to the production of lepton pairs by virtual photons in the Coulomb fields of nuclei and atomic electrons, respectively. "Pairs" and "triplets" refer to the corresponding processes induced by real photons.
[10] J. Bohm, V. G. Grishin, M. M. Muminov, and V. D. Ryabtsov, Joint Institute for Nuclear Research Report No. JINR-P1-3143, 1967 (unpublished).
[11] A. Browman, B. Grossetête, and D. Yount, Phys. Rev. **151**, 1094 (1966).

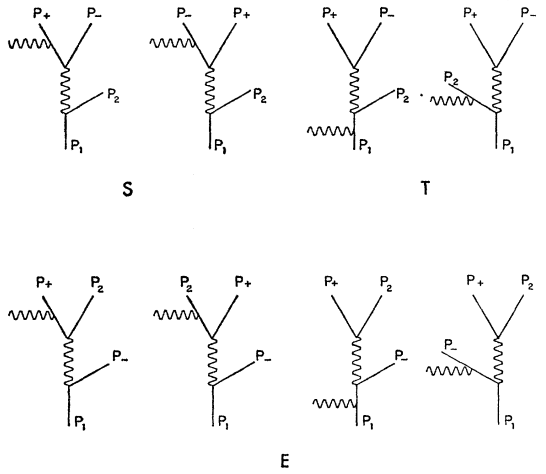

FIG. 1. Feynman diagrams for trident production. The first two graphs correspond to spacelike momentum transfers, while the second two correspond to timelike transfers. The last four are exchange diagrams appropriate when the incident particle is an electron or positron.

to as BGY, on positron-electron scattering at 180°. In the 180° scattering experiment, the trident and pair processes were initiated by incident positrons, and they produced a background of electrons at 0° which was of order 1% of the recoil-electron signal. A crude check of this background was made by detecting positrons with the spectrometer still at 0° and with electrons incident, but no attempt was made to separate the trident and pair contributions.

Since trident production and quartet production are linear in target thickness while pair production and triplet production are quadratic, the direct and cascade processes with incident electrons can be separated by varying the target thickness. Similarly, production in the field of an atomic electron[12] is linear in atomic number Z, while production in the field of a nucleus is quadratic. Thus tridents from nuclei can be separated from quartets from atomic electrons by varying Z, and pairs from nuclei can be separated from triplets from atomic electrons in the same way.

In this experiment, we have used targets having thicknesses in radiation lengths of $t_1 \approx 0.001 X_0$ and $t_2 \approx 0.02 X_0$ to separate the direct and cascade processes, and we have taken data with beryllium ($Z=4$), aluminum ($Z=13$), and platinum ($Z=78$) targets to separate the electron and nuclear contributions. The cross-section differential in the final positron energy $d\sigma/dE$ was measured at a number of points in the range $0.80E_0 \leq E \leq 1.02E_0$. The statistical precision is about 5% for the direct process and about 2% for the double process at most points; the systematic errors are estimated to be about 2% in each case.

[12] J. Joseph and F. Rohrlich, Rev. Mod. Phys. **30**, 354 (1958).

II. THEORY

In this section we list a number of formulas to be compared later with the experimental results. While the bremsstrahlung and pair production expressions are expected to be precise, the formulas given for trident production contain various approximations which are not necessarily valid for our experimental conditions. The trident expressions also contain unevaluated constants, which we have adjusted to optimize the fit with the data.[13]

Bhabha[14] in 1935 and Racah[15] in 1937 were among the first to study trident production. Bhabha showed that within the accuracy of his calculations the Weizsäcker-Williams approximation gives the same result as the usual quantum-mechanical treatment. In this approximation, one essentially compares the spectrum of the virtual quanta associated with an incident electron with a real bremsstrahlung spectrum, while the cross section for pair production is assumed to be the same for the virtual and real γ rays.

The Bhabha trident cross section can be expressed as[16]

$$X(E_0,k,\mu)=(8/\pi)\alpha^2(N/A)Z^2r_e^2H(E_0,k,\mu)\,, \tag{1a}$$

$$H(E_0,k,\mu)=\frac{1}{3k}(1+\tfrac{1}{2}\mu^2)\ln\left[\frac{C_1}{(k/E_0)}\right]L_B\,, \tag{1b}$$

$$\mu=(2E-k)/k\,, \tag{1c}$$

$$L_B=\ln[C_2k(1-\mu^2)/4mc^2] \text{ for no screening,} \tag{1d}$$

and

$$L_B=\ln[C_2/3\alpha Z^{1/3}] \text{ for complete screening,} \tag{1e}$$

where $X(E_0,k,\mu)dkd\mu dx$ is the probability that a single electron of energy E_0, on traversing a thickness dx g/cm^2 of matter, will produce a pair with total energy between k and $k+dk$, with positron energy E, and with a value of μ between μ and $\mu+d\mu$. In this expression, α is the fine-structure constant, N is Avogadro's number, A is the atomic weight of the target nucleus, Z is the atomic number, mc^2 is the electron mass, and r_e is the classical electron radius. The symbols C_1 and C_2 represent constants of order unity.

The virtual photon spectrum contributes to Eqs. (1a)–(1e) the factor

$$N\left(\frac{k}{E_0}\right)\frac{dk}{E_0}=2\pi\alpha\frac{dk}{k}\ln\left[\frac{C_1}{k/E_0}\right]. \tag{1f}$$

The experimental result of Camac[8] can be expressed as $C_1=1.6\pm0.2$, which is "in agreement with the

[13] Precise calculations containing no undetermined constants are presently being carried out for this experiment by Brodsky [S. Brodsky (private communication)].

[14] H. J. Bhabha, Proc. Roy. Soc. (London) **152**, 559 (1935).

[15] G. Racah, Nuovo Cimento **14**, 93 (1937).

[16] B. Rossi, *High Energy Particles* (Prentice-Hall, Inc., Englewood Cliffs, N. J., 1952).

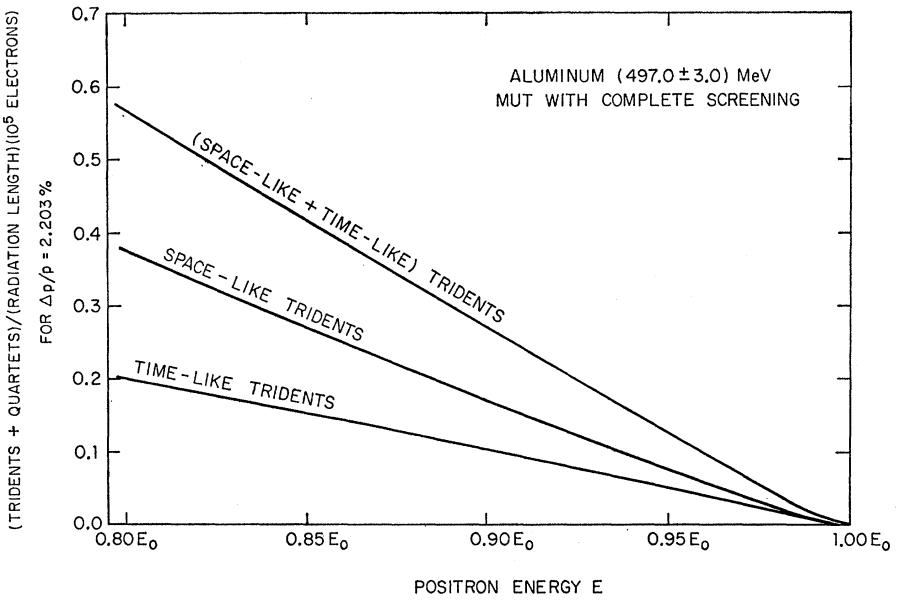

FIG. 2. Spacelike and timelike positron energy spectra calculated by MUT for trident production with complete screening.

Weizsäcker-Williams approximation." Unfortunately, since $k/E_0 \sim 1$, the logarithmic factor in Eq. (1f) is approximately $\ln[C_1/(k/E_0)] \sim (C_1-1)-[(k/E_0)-1] \sim C_1-(k/E_0)$. The experimental error in C_1 thus amounts to an uncertainty of about $\pm 0.2/0.8 \sim \pm 25\%$ of the trident cross section, while the predicted rate depends strongly upon the value for C_1 that one happens to choose. (The rate varies slowly with C_2 which can be set equal to unity for our purposes.)

The most complete published calculation of the trident rate for our experimental conditions is that of Murota, Ueda, and Tanaka,[17] hereafter referred to as MUT. They considered the first four Feynman diagrams given in Fig. 1, but ignored the four exchange diagrams appropriate when the incident particle is an electron or positron. The first two graphs correspond to spacelike momentum transfer (S) while the second two correspond to timelike transfers (T).

Surprisingly, the calculations of MUT indicate (Fig. 2) that for our experimental conditions the timelike momentum transfers contribute more than one-third of the net differential cross section, a result that is inconsistent with a naive application of the Weizsäcker-Williams approach and its tacit assumption of spacelike dominance. On the other hand, a fortuitous agreement of the Bhabha and MUT predictions can always be obtained for a given element at a given electron and positron energy simply by adjusting the parameter C_1 in the virtual photon spectrum of Eq. 1(f).

Unfortunately, MUT does not give an expression for the interference terms between the spacelike and timelike diagrams. Thus in our experimental region, where the timelike and spacelike diagrams are comparable, the theory of MUT is uncertain because of the neglect of both the interference and the exchange diagrams.[18] While these uncertainties may be even larger than the $\pm 25\%$ uncertainties in the Bhabha formula with $C_1 = 1.6 \pm 0.2$, we have used MUT in most of our calculations. Like the Bhabha formula, the expression of MUT is amenable to numerical integration over the intermediate photon energy as well as over the momentum acceptance of the spectrometer.

The formula given by MUT for the spacelike terms when the target thickness is in g/cm² is

$$\sigma_s = \frac{2}{\pi}\frac{N}{A}\alpha^2 Z^2 r_e^2 dE_+ dE_- L \times \left\{\left[\frac{E_+^2+E_-^2}{k^4}\left\{(1+\tfrac{4}{3}x)\ln\left(1+\frac{1}{x}\right)-\tfrac{4}{3}\right\}+\frac{2}{3}\frac{E_+E_-}{k^4}\left\{(1+2x)\ln\left(1+\frac{1}{x}\right)-2\right\}\right]\times\frac{E_1^2+E_2^2}{E_1^2}\right.$$
$$\left.+\frac{8}{3}\frac{E_+E_-}{k^4}\frac{1}{1+x}\frac{E_2}{E_1}+\left[\frac{E_+^2+E_-^2}{k^4}\left\{\frac{1}{3}\frac{1}{1+x}+\frac{1}{x}-\tfrac{4}{3}\ln\left(1+\frac{1}{x}\right)\right\}+\frac{2}{3}\frac{E_+E_-}{k^4}\left\{\frac{1}{1+x}+\frac{1}{x}-2\ln\left(1+\frac{1}{x}\right)\right\}\right]\frac{k^2}{E_1^2}\right\}, \quad (2a)$$

where E_1 is the incident electron energy ($E_1=E_0$), E_2 is the final electron energy ($E_2=E_0-k$), E_+ and E_- are the energies of the positron and electron from the pair and k their sum ($k=E_++E_-=E_1-E_2$), and

[17] T. Murota, A. Ueda, and H. Tanaka, Progr. Theoret. Phys. (Kyoto) **16**, 482 (1956).

[18] The interference between the timelike and spacelike diagrams is expected to be of order 10–20% of the net cross section. The exchange diagrams lower the trident cross section by about 25% [S. Brodsky (private communication)].

where

$$x=E_+E_-/E_1E_2, \tag{2b}$$

$$L=\ln\left[\frac{2C_3E_+E_-}{kmc^2(1+x)^{1/2}}\right]-1 \quad \text{for no screening}, \tag{2c}$$

and

$$L=\ln\left[\frac{C_3(1+x)}{\alpha Z^{1/3}}\right] \quad \text{for complete screening}. \tag{2d}$$

In this expression, the terms proportional to $(E_1^2+E_2^2)/E_1^2$ and E_2/E_1 correspond, respectively, to the process in which the spin of the incident particle does not flip and the direction of polarization of the virtual photon is transverse, and the process in which the spin of the incident particle does not flip but the direction of polarization of the virtual photon is longitudinal. The term proportional to k^2/E_1^2 corresponds to the process in which the spin flips and the virtual photon is transversely polarized. In our experimental region, the dominant terms are for no spin flip and for transverse polarization. This suggests that the Weizsäcker-Williams result should be a good approximation to the spacelike cross section.

The expression for the timelike diagrams is similar to that for the spacelike diagrams:

$$\sigma_T=\frac{2}{\pi}\alpha^2\frac{N}{A}Z^2r_e^2dE_+dE_-L'\frac{E_+^2+E_-^2}{E_1^2}\times\frac{E_1^2+E_2^2}{k^4}\left[\left\{\left(1+\frac{4}{3x}\right)\ln(1+x)-\tfrac{4}{3}\right\}-\frac{2}{3}\frac{E_1E_2}{k^4}\left\{\left(1+\frac{2}{x}\right)\ln(1+x)-2\right\}\right], \tag{3a}$$

where

$$L'=\ln\left[\frac{2C_3E_1E_2}{mc^2k(1+1/x)^{1/2}}\right]-1 \quad \text{for no screening}, \tag{3b}$$

and

$$L'=\ln\left[\frac{C_3(1+1/x)^{1/2}}{\alpha Z^{1/3}}\right] \quad \text{for complete screening}. \tag{3c}$$

Looking now at the MUT equations, we see that they contain only one constant $C_3\sim1$, instead of the two constants $C_1\sim C_2\sim1$ of the Bhabha formula. Since $E_+\sim E_1$ $(E\sim E_0)$ and since $E_-\sim E_2$ $(\langle k-E\rangle_{\rm av}\sim\langle E_0-k\rangle_{\rm av}$ in the integration over k, the parameter x given by Eq. (2b) has an effective value near unity. The expressions $C_3(1+x)\sim C_3(1+1/x)^{1/2}\sim1$ can then be associated with C_2 of the Bhabha formula, while the sensitive parameter C_1 has disappeared. To the extent that the omission of the interference and exchange diagrams is justified, the MUT equations provide unambiguous predictions that are not very sensitive to the value of the single undetermined constant C_3.

The cross section for bremsstrahlung integrated over all angles can be expressed in the form[19]

$$\frac{d\sigma(k)}{dk}=\alpha(N/A)Z^2r_e^2k^{-1}E_1^{-2}\times[(E_1^2+E_2^2)2\Gamma_1-4E_1E_2\Gamma_2], \tag{4a}$$

where the target thickness is again in g/cm^2 and where E_1 is the incident electron energy $(E_1=E_0)$, E_2 is the final electron energy $(E_2=E_0-k)$, and k is the photon energy.

The most precise calculations of the screening functions Γ_1 and Γ_2 involve numerical integrations[19] over the atomic form factors,[20] but for simplicity we have used the expressions given by Ref. 21:

$$2\Gamma_1=\phi_1-\tfrac{4}{3}\ln Z-4f(Z), \tag{4b}$$

$$4\Gamma_2(\tfrac{3}{2})=\phi_2-\tfrac{4}{3}\ln Z-4f(Z), \tag{4c}$$

where ϕ_1 and ϕ_2 are the screening functions of Bethe and Heitler[22] and $f(Z)$ is the Coulomb correction term of Bethe and Maximon[23,21]:

$$f(Z)=1.202X-1.0369X^2+1.008X^3/(1+X), \tag{4d}$$

$$X=(Z/137)^2 \quad \text{for} \quad Z>1. \tag{4e}$$

The contribution from electron-electron bremsstrahlung is calculated from [12,24]

$$d\sigma=\alpha(N/A)Zr_e^2k^{-1}E_1^{-2}[(E_1^2+E_2^2)2\Gamma_3-4E_1E_2\Gamma_4], \tag{4f}$$

where

$$2\Gamma_3=\psi_1-4-(8/3)\ln Z, \tag{4g}$$

$$4\Gamma_4(\tfrac{3}{2})=\psi_2-(10/3)-(8/3)\ln Z, \tag{4h}$$

and where ψ_1 and ψ_2 are the screening functions for electron-electron bremsstrahlung. The formulation just described is contained in the thick-target bremsstrahlung program of Early,[25] based on a similar program of Alvarez[26] and the review article of Koch and Mortz.[24]

The cross section for pair production integrated over all angles can be expressed in the form[19]

$$\frac{d\sigma(E_1)}{dE_1}=\alpha(N/A)Z^2r_e^2k^{-1}k^{-2}\times[(E_1^2+E_2^2)2\Gamma_1+4E_1E_2\Gamma_2], \tag{5a}$$

where E_1 is now the positron energy $(E_1=E)$, E_2 is the electron energy $(E_2=k-E)$, and k is the incident

[19] A. Sorensson, Nuovo Cimento **38**, 745 (1965).
[20] H. P. Hanson, F. Herman, J. D. Lea, and S. Skillman, Acta Cryst. **17**, 1040 (1964).
[21] H. Davies, H. A. Bethe, and L. C. Maximon, Phys. Rev. **93**, 788 (1954).
[22] H. A. Bethe and W. Heitler, Proc. Roy. Soc. (London) **A146**, 83 (1934).
[23] H. A. Bethe and L. C. Maximon, Phys. Rev. **93**, 768 (1964).
[24] H. W. Koch and J. W. Motz, Rev. Mod. Phys. **31**, 920 (1959).
[25] R. A. Early, Stanford Linear Accelerator Center Technical Note No. TN-66-15, 1966 (unpublished).
[26] R. A. Alvarez, Stanford High-Energy Physics Laboratory Report No. HEPL-228, 1961 (unpublished).

photon energy. The expression for pair production in the field of an electron is analogous to Eq. (4f) with the change of variable and sign change implicit in Eq. (5a). As indicated by the notation, the corresponding screening functions are the same for bremsstrahlung and pair production.[19] We have therefore obtained a pair-production program by simply changing the appropriate variables and a sign in the bremsstrahlung program. The bremsstrahlung and pair production programs are expected to be accurate to 2–3% so that predictions for the cascade process should be uncertain by no more than about 5%.

To test the sensitivity of the experiment, it will be interesting to compare the experimental results with the Bethe-Heitler[22] cross sections for pair production in the no-screening and complete-screening limits as well as with the more recent predictions derived from the thick-target bremsstrahlung program. The Bethe-Heitler cross section can be expressed as[16]

$$\frac{d\sigma(k,E)}{dE}=4\alpha(N/A)Z^2r_e^2k^{-1}G(k,V). \tag{5b}$$

$$G(k,V)=[V^2+(1-V)^2+\tfrac{2}{3}V(1-V)]\times\left[\ln\left(\frac{2k}{mc^2}V(1-V)\right)-\tfrac{1}{2}\right] \tag{5c}$$

for no screening, and

$$G(k,V)=[V^2+(1-V)^2+\tfrac{2}{3}V(1-V)]\ln(183Z^{-1/3})-\tfrac{1}{9}V(1-V) \tag{5d}$$

for complete screening, where

$$V=(E+mc^2)/k. \tag{5e}$$

Here k is the incident photon energy and E is the positron energy.

III. APPARATUS

Figure 3 shows the experimental setup in vertical section. As mentioned in the Introduction, the geometry and apparatus were the same, with some small exceptions, as those used by BGY in the 180° positron-electron scattering experiment. The rates for trident and pair production were, however, only about 1% of the rates in the scattering experiment. Furthermore, the separation of the direct and cascade processes required that somewhat thinner targets be used, and this reduced the rate per incident electron still further. One count per 10^9 electrons incident is a typical value for the trident spectrum. Because of the smaller signal, our sensitivity to certain backgrounds was two to three orders of magnitude worse than previously; an "empty-target" substraction was essential, and the spurious rate was large. As a precaution against fluctuations, the thin-target R_1 and empty-target R_0 data were taken on a number of cycles down the recoil positron spectrum.

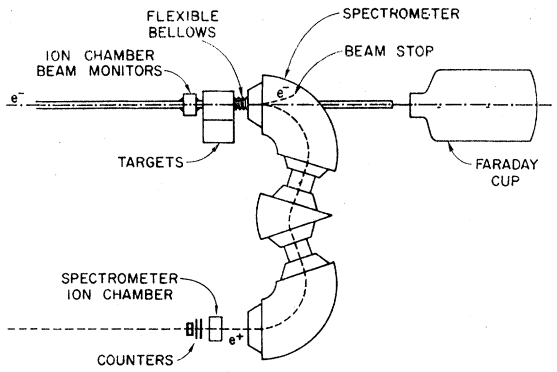

FIG. 3. Experimental setup in vertical section. Momentum-analyzed electrons entered from the left and were incident on the ion-chamber beam monitors and various targets. Recoil positrons from pair, triplet, trident, and quartet production were momentum-analyzed by the three-magnet spectrometer set at 0° and were detected by counters located at the focus of the spectrometer. The Faraday cup and spectrometer ion chamber were used in various tests described in the text.

In Fig. 3, momentum-analyzed electrons from the Orsay linear accelerator passed through thin ionization-chamber intensity and position monitors and were incident on various targets located at the center of rotation of the double-focusing, zero-dispersion spectrometer.[27] Positrons from tridents, quartets, pairs, and triplets were momentum-analyzed with the spectrometer set at 0° and were detected by two plastic scintillators and by a Lucite Čerenkov counter used to check that possible backgrounds involving recoil protons were negligible. Another ion chamber, placed just in front of the counters, was used in studies of the spectrometer momentum and angular acceptance as well as in the target thickness measurements described in detail in the next section. The scattering chamber surrounding the targets was connected directly to the vacuum chamber of the spectrometers and extended to the entrance window. Flexible bellows were used between the chamber and the spectrometer to permit changes in spectrometer angle of about ±3°. The ion chamber beam monitors were calibrated with the "1-GeV" Orsay Faraday cup[28] when the field in the spectrometer was zero.

The three-magnet deviation system[29] used to momentum-analyze the incident beam was monitored with an NMR probe located in the first analyzing magnet. The momentum setting was 498.5±1.5 MeV/c, and the momentum slits were set at $\Delta p/p=0.5\%$. The beam shape was defined by a 1-cm×1-cm collimator located just in front of the first analyzing magnet. With no quadrupole focusing, this results in a parallel beam

[27] B. Milman, L'Onde Electrique **42**, 310 (1962).
[28] The "1-GeV" Faraday cup is similar in design to the "500-MeV" Orsay Faraday cup described by D. Isabelle, L'Onde Electrique **42**, 354 (1962).
[29] B. Milman, Nucl. Instr. Methods **20**, 13 (1963). The recent data on the beam angular divergence were supplied by B. Milman (private communication).

(angular divergence less than 2×10^{-4} rad)[29] having roughly the same dimensions as the collimator. A second collimator located just in front of the last analyzing magnet was used to "scrape" the beam and reduce beam halo. The size of this collimator, 2 cm×2 cm, was chosen experimentally to minimize the backgrounds which result when a small fraction of the primary beam hits the relatively thick material outside the normal beam line.

Precise measurements of the momentum acceptance $\Delta p/p$ of the spectrometer were carried out by BGY at 500 MeV/c, as well as at 200 MeV/c, with the momentum slits set at 7.054±0.004 cm. We have used the same settings on the remote slit control unit and have obtained a separation of 7.048±0.004 cm, in good agreement with BGY. The momentum acceptance is then

$$\Delta p/p(500\ \text{MeV}/c)=(2.203\pm0.008)\ \%, \quad (6)$$

as determined by BGY. A check of $\Delta p/p$ was also obtained during the target-thickness studies described in Appendix A; the result was (2.210±0.024) %, which is consistent with BGY within errors of about 1% of $\Delta p/p$. The incident energy determined by the spectrometer was 495.5±0.6 MeV. We shall take the incident energy to be the average of the deviation system and spectrometer values and assign an error of ±0.6%, as in BGY:

$$E_0=497.0\pm3.0\ \text{MeV}. \quad (7)$$

We should mention two more differences in this experiment and that of BGY. First, we have decreased the thickness t_0 of the ion chamber beam intensity and position monitors from about $0.002X_0$ to about $0.001X_0$. This has been accomplished by using 0.0015-in. Mylar entrance and exit windows instead of the 0.004-in. aluminum windows of BGY. The slow diffusion of hydrogen through the windows precludes the use of a sealed container, and instead we have flowed hydrogen through the chamber at ambient temperature and pressure. As before, a "thick" and a "thin" ion chamber, as well as a beam position indicator, were contained within the same hydrogen volume; the two ion chambers had different ion recombination characteristics, and the ratio of their outputs provided a sensitive check that saturation did not occur.[30]

Unlike positron-electron scattering with its two-body final state, trident, quartet, pair, and triplet production are not constrained kinematically to be within a certain small angle when the incident and final momenta have a given set of values. Nevertheless, the characteristic angle, mc^2/E_0, for these processes is small compared to the horizontal angular acceptance of the spectrometer (typically $\pm18mc^2/E_0$); it is very small compared to the vertical acceptance, which is about five times the horizontal acceptance. Thus only a few percent of the trident-plus-quartet rate is outside of the angular acceptance with the spectrometer at 0°, and less than 1% of the pair-plus-triplet rate is lost. Detailed experimental and theoretical studies of these losses were carried out and are described in Sec. IV on data analysis; an experimentally determined correction increases the effective angular acceptance to $\pm54mc^2/E_0$.

A central problem in this experiment is the determination of the target thicknesses. Basically there are six targets, one thin ($t_1\approx0.001X_0$) and one thick ($t_2\approx0.020X_0$) target for each of the three elements, beryllium, aluminum, and platinum. In addition, the two ion chambers and beam-position monitor are in the beam throughout the data run, and these contribute aluminum foils, Mylar windows, and hydrogen gas comparable in thickness with the thin targets ($t_0\approx0.001X_0$). The nature of the problem can be appreciated by noting that the thin platinum target is only 0.00733 g/cm² thick or about 3 μ. Even the aluminum target at 0.02625 g/cm² or 100 μ is very thin by most standards.

We have determined the target thicknesses first of all by weighing each 2-in.×2-in. sample on a sensitive analytical balance and by measuring the linear dimensions and thus the area with a micrometer. This procedure is straightforward and leads to errors in the *average* thickness of less than ±0.4%. The target uniformity and the effective thickness for a 1-cm² beam spot are still in doubt, however, at least in cases of the thinnest targets.

During the data run, a sub-experiment was performed in which the relative intensity of the "bremsstrahlung tail" was measured for each target, including the beam ion chamber. In this sub-experiment, described in Appendix A, the spectrometer was at 0° with the field set for electrons of somewhat lower energy (nominally $0.96E_0$ and $0.92E_0$) than the incident electron beam energy. The transmitted electrons were monitored with ion chambers located at the output of the spectrometer, and the ratio of transmitted to incident particles for a setting on the bremsstrahlung tail was roughly proportional to the target thickness in radiation lengths.

Our intention was to use the bremsstrahlung technique to determine the ratios of the thin-to-thick target thickness for each element. A ratio experiment of this type avoids uncertainties in the absolute magnitude of the bremsstrahlung as well as those associated with the Z dependence. The corrections which must be made for the differences in target thickness, particularly ionization and multiple photon emission, are 10% or less and can be checked experimentally by comparing the ratios at different settings on the bremsstrahlung tail. The measurements themselves require integration times of about 100 sec per point and are reproducible to better than 1%, even though the rate in the spectrometer ion chamber is, in some cases, more than three orders of magnitude lower than the incident beam intensity. The "random" measurement error can be

[30] D. Yount and J. Pine, Phys. Rev. **128**, 1842 (1962).

reduced well below 1% and can be estimated by taking a number of integrations and combining the results statistically. The most attractive feature of the bremsstrahlung technique is that it provides a direct test of the target uniformities and target thicknesses under the actual conditions of the data run.

IV. DATA ANALYSIS

As discussed in Appendix B, it is possible to extract the trident rate T, the pair rate P, and the background B from the three measured rates R_0, R_1, and R_2 for the empty target, the thin target, and the thick target, respectively. A detailed analysis indicates that the background results mainly from less than 10^{-4} of the primary beam being outside the 5-cm-diam clear region and passing through spurious target material of greater than $0.13X_0$ effective thickness. The analysis shows that this background, like several others considered, can be subtracted out so that T and P depend only upon the differences (R_1-R_0) and (R_2-R_0) and upon the target thicknesses t_0, t_1, and t_2.

The first step in the data analysis was the determination of the number of electrons incident at each point. The gain of the "thin" ion chamber was 11.73 ± 0.08 ions per incident electron, as determined from five intercalibrations of the ion chamber and Faraday cup during the run. The assigned error takes into account the small absolute uncertainties in the value of the integrator capacitors and in the "1-GeV" Orsay Faraday cup efficiency (BGY) as well as the larger changes in ion chamber gain with temperature and pressure. The number of electrons incident at each point was then calculated from the gain, the integrated charge, the absolute value of the integrator capacitor used, and the charge of the electron.

The counting rate corrections were calculated from the scaler resolving times and the duration of the accelerator beam spill, which was continuously monitored throughout the run. Counting-rate corrections were typically 1% or less and could be made to an accuracy of about 20% of the correction. This corresponds to an uncertainty of 0.2% or less in the counting rates and is negligible. The corrected number of counts per incident electron was then computed for each point.

The corrections for the losses due to bremsstrahlung in the target were made by folding together the bremsstrahlung cross section of Eqs. (4a)–(4h), the experimental energy resolution, and a linear approximation to the trident or pair cross sections. The linear function was simply a constant times the difference in incident and final energies (E_0-E). The correction was the percent change in the counting rate before and after the fold was carried out, and it did not depend upon the normalization.

For the empty-target R_0 and thin-target R_1 measurements, trident production was assumed to dominate. The effective target thickness in this case was the actual thickness since either the incident electron or the final positron passed through each increment of target thickness. Because the incident and final energies were similar, the bremsstrahlung correction was not very sensitive to whether the radiation occurred before or after the production process. An average of the two cases reduced the uncertainty still further. The magnitude of the bremsstrahlung correction for R_0 and R_1 was 1% or less.

For the thick-target R_2 measurements, pair production was assumed to be the dominant process. The effective target thickness for bremsstrahlung losses as well as for Landau straggling, ionization, multiple scattering, etc., was less than the true thickness in the cascade process because of the finite distance traveled by the intermediate photon. On the average, the incident electron penetrated $\frac{1}{3}$ of the target thickness, the intermediate photon was present during the second $\frac{1}{3}$, and the positron passed through the last $\frac{1}{3}$. The effective target thickness was then $\frac{2}{3}$ of the actual thickness, as far as these corrections were concerned. The magnitude of the thick-target bremsstrahlung losses was 7–14%, and the correction was made to an accuracy of about 10% of this, i.e., to better than $\pm1.4\%$ of R_2.

The correction for the losses due to Landau straggling was similar to that for bremsstrahlung in the target except that the straggling was an order of magnitude smaller. This correction was also made directly to R_0, R_1, R_2 before the trident T and pair P rates were computed. There is, of course, some doubt about how the various corrections to R_0 and R_1 should be made when the background B is large. Such doubt is diminished by the smallness of these corrections in the thin-target cases and by the smallness of the fractional background in the thick-target cases.

Prior to the data run, a detailed calculation was made of the "multiple-scattering" losses in the thick target, pair production case. In this calculation, the bremsstrahlung and pair-production angular distributions were folded together, assuming that the photon had an energy halfway between that of the incident electron and the final positron. The result at this stage was an angular distribution for the cascade process in terms of horizontal θ_H and vertical θ_V scattering angles. A second two-dimensional integration was made over the cascade angular distribution and a Gaussian multiple-scattering function. Since the spectrometer angular acceptance was about five times as large vertically as horizontally, the final angular distribution was projected into the horizontal scattering plane. The multiple-scattering losses could then be estimated to a calculational accuracy of perhaps 10–20% by integrating over the final projected "cross section" in the region outside of the horizontal spectrometer angular acceptance. Some of the results of this calculation are plotted in Fig. 4.

The primary purpose of the multiple-scattering calculation just described was to verify *a priori* that the

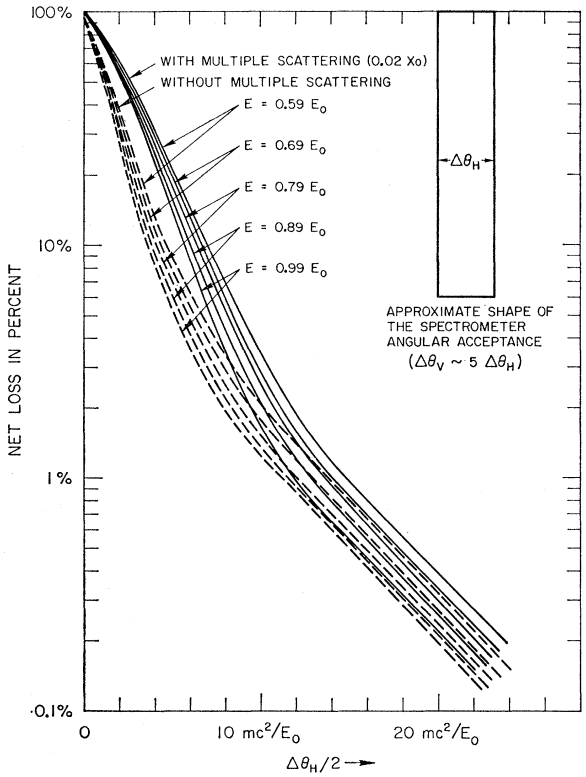

FIG. 4. Theoretical angular distributions for bremsstrahlung followed by pair production. The final angular distributions projected onto the horizontal scattering plane have been integrated over the horizontal angular acceptance of the spectrometer to obtain the loss in percent with no multiple scattering and with multiple scattering in targets of $0.02X_0$ thickness.

multiple-scattering losses would not be so large as to jeopardize the experiment. The calculation indicated typically that only about 0.5% of the cascade events for an incident electron of $E_0=500$ MeV and for a final positron of $0.59E_0<E<0.99E_0$ would be outside of the $\pm 18mc^2/E_0$ horizontal angular acceptance. The result is changed very little by the 1 cm $\sim 5mc^2/E_0$ beam-spot diameter. No angular distribution for the trident process was available, but the similarity of the direct and cascade processes suggested that the multiple-scattering losses in the thin-target, trident production case would also be small. If so, the actual correction could be made experimentally by measuring the counting rate as a function of spectrometer angle near 0° for each target.

We should mention here that the multiple-scattering corrections were observed directly in the rates R_0, R_1, and R_2 and were then applied to the difference in these rates. In particular, the background B could be subtracted out, as usual; its angular distribution did not seriously affect the measurements as long as the background was stable and as long as (R_1-R_0) and (R_2-R_0) could be determined with the desired statistical accuracy.

TABLE I. Multiple-scattering corrections.

E	$0.98E_0$	$0.95E_0$	$0.90E_0$	$0.80E_0$
$\Delta\theta_H$ (mc^2/E_0)	33.8±1.6	35.6±1.0	36.4±1.0	41.6 ±1.0
$\delta_{MS}(R_1-R_0)$ (%)	3.3±1.5	3.0±1.3	3.6±1.2	2.4 ±1.0
$\delta_{MS}(R_2-R_0)$ (%)	···	···	···	0.51±0.09

The angular distribution obtained for R_0 and R_1 at $0.95E_0$ is shown in Fig. 5. The full width of the curve at half-maximum $[(2.10\pm0.06)° \leftrightarrow (35.6\pm1.0)mc^2/E_0$ in this case] is a direct measurement of the horizontal angular acceptance of the spectrometer $\Delta\theta_H$, while the vertical acceptance in this rectangular approximation is effectively 180° ($\Delta\theta_V\sim 5\Delta\theta_H$). The tails of the distribution indicate the fraction of the events still within the angular acceptance when the spectrometer is rotated a given angle away from 0°.

Ideally, the multiple-scattering correction is made by summing the rates measured when the spectrometer is rotated to $\pm\Delta\theta_H$. In effect, this extends the angular acceptance to about $\pm 54mc^2/E_0$. In practice, since $\Delta\theta_H$ and the beam centering were not precisely known *a priori*, the actual points were near $\pm\Delta\theta_H$ and not exactly at these settings. The multiple-scattering corrections were therefore determined by extrapolating from the actual to the ideal points using the calculated angular distributions for the cascade process. This procedure depends only upon the local shape of the calculated distribution, and the extrapolation spans only a few mc^2/E_0 in most cases. Furthermore, points taken on either side of the ideal setting extrapolated to the same value within the statistical errors assigned. The complete angular distributions were obtained only for the aluminum targets since check points with platinum and beryllium at the steep edges of the distribution were in the same ratio to the aluminum as the points at 0°.

The multiple-scattering corrections determined experimentally are tabulated for various positron energies below. The angular distribution of Fig. 4 broadens slowly with decreasing positron energy, but at the same time, the spectrometer angular acceptance increases as the magnet iron comes out of saturation. The result is that the multiple-scattering losses are fairly constant over the positron spectrum. On the basis of the data in Table I, we have assigned a multiple-scattering correction of $(+2.9\pm0.7)$% for (R_1-R_0) and $(+0.4\pm0.2)$% for (R_2-R_0) for all momenta in the range from $0.80E_0$ to $0.98E_0$. Evidently, the trident angular distribution is much broader than the pair distribution.

Because of ionization, the spectrum obtained for each target is shifted to lower energies by an amount ΔE_I which depends upon the target thickness in g/cm². The result is that values of R_0, R_1, and R_2 measured at a given spectrometer setting do not correspond to the same positron momentum. Before the trident T and pair P rates can be extracted by means of the equations given in Appendix B, the values of R_0, R_1, and R_2

must be corrected to a common energy or momentum setting.

The values of ΔE_I in MeV for each target are given in Appendix A for the case of an electron or positron which passes through the full thickness of material. In calculating T, the rates for R_0 and R_2 were shifted relative to R_1 by the equations

$$R_0 \rightarrow R_0\left[1+\left(\frac{\Delta E_I(t_0)-\Delta E_I(t_1)}{E_0-E}\right)\right], \quad (8a)$$

$$R_2 \rightarrow R_2\left[1+\left(\frac{\frac{2}{3}\Delta E_I(t_2)-\Delta E_I(t_1)}{E_0-E}\right)\right]. \quad (8b)$$

In calculating P, the rates for R_0 and R_1 were shifted relative to R_2 by means of the expressions

$$R_0 \rightarrow R_0\left[1+\left(\frac{\Delta E_I(t_0)-\frac{2}{3}\Delta E_I(t_2)}{E_0-E}\right)\right], \quad (9a)$$

$$R_1 \rightarrow R_1\left[1+\left(\frac{\Delta E_I(t_1)-\frac{2}{3}\Delta E_I(t_2)}{E_0-E}\right)\right]. \quad (9b)$$

The quantity (E_0-E) in the above equations is determined in terms of the spectrometer momentum only and represents the displacement in MeV down from the spectrum intercept. The factor of $\frac{2}{3}$ multiplying $\Delta E_I(t_2)$ is equivalent to the assumption made earlier that the thin-target rates are dominated by tridents while the thick-target rates are due mainly to pairs. As usual, this is a good assumption in the thick-target R_2 case where tridents contribute about 15% to the observed rate. In the thin target R_0, R_1 cases, the values of ΔE_I are small anyway.

In the sense that the cascade process P is a background in the determination of the direct process T (and conversely), the ionization is actually a second-order correction which is small except in the vicinity of the spectrum intercept, where the statistical errors are large. The difficulties which arise in Eqs. (8a) and (8b) and (9a) and (9b) when (E_0-E) approaches zero were removed artificially by requiring $(E_0-E)\geq 10$ MeV/c, this being roughly the spectrometer momentum resolution at 500 MeV. The largest ionization correction is about 13% for the thick beryllium target rate, e.g., for R_2 in the determination of $T(Z=4)$. The net correction to the extracted value of T in this case is of order 13%/3$\sim$4% in the region within 2% of the intercept and less than 2% at a setting 5% down from the intercept. The effect on P is still less since the direct process contributes only about 15% of the rate with R_2.

A net correction of +0.32% for positron annihilation and for bremsstrahlung losses in the counters was made to R_0, R_1, and R_2 at each point on the spectrum. A correction of this type does not change the relative importance of the direct and cascade processes but is necessary in determining the absolute rates.

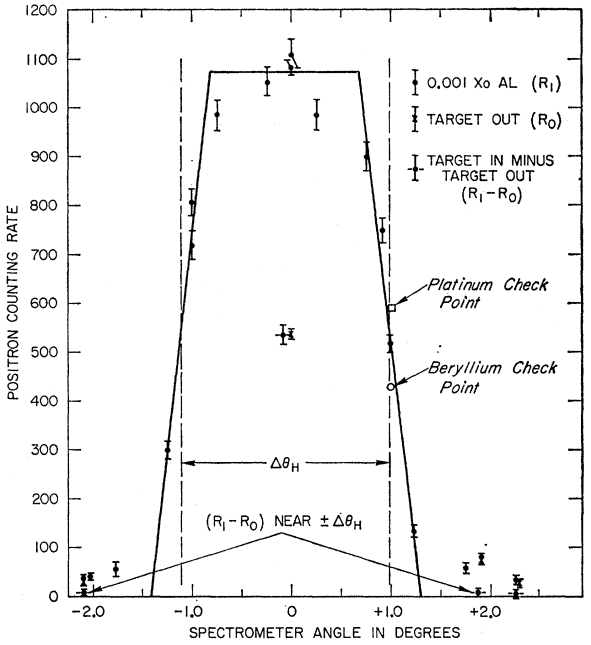

FIG. 5. Experimental angular distributions for the empty-target rate R_0 and thin-target rate R_1 at a positron energy of $0.95E_0$. The full width at half-maximum gives the horizontal angular acceptance of the spectrometer, while the tails of the distribution indicate the fraction of the events still within the angular acceptance when the spectrometer is rotated a given angle away from 0°. The experimental multiple-scattering correction extends the effective angular acceptance from $\pm 18mc^2/E_0$ to about $\pm 54mc^2/E_0$. Similar curves were obtained at $0.80E_0$, $0.90E_0$, and $0.98E_0$ for R_1 and R_0 and at $0.80E_0$ for the thick-target rate R_2.

Protons from photonuclear or electronuclear interactions can have momenta higher than 500 MeV/c and are not distinguished from positrons in this experiment. A generous upper limit for the electronuclear process can be obtained from the formulas of Ref. 31 and from the electronuclear data of Ref. 32 by assuming that all protons of the proper momentum are within the angular acceptance of the spectrometer. The limit calculated for the thin aluminum target at 400 MeV/c is 0.12 protons/(10^{10} electrons incident). The limit is finite but a factor of about 6 smaller at 500 MeV/c. These limits correspond to about 0.3% of the trident rate at $0.80E_0$ and about 0.6% at $0.98E_0$.

The photoproton background is less important than the electroproton background since the equivalent radiator for electronuclear interactions ($\sim 0.03X_0$) is much thicker than the equivalent radiator for electroproduction pairs, i.e., tridents ($0.003X_0$). The proton backgrounds in percent may be larger for beryllium than for aluminum, but they should not be more than $Z_{Al}/Z_{Be}=13/4\sim 3$ times larger.

[31] J. A. Thie, C. J. Mullin, and E. Guth, Phys. Rev. 87, 962 (1952).

[32] W. R. Dodge, doctoral dissertation, Stanford University, Stanford, California, 1961 (unpublished); Stanford High-Energy Physics Laboratory Report No. HEPL-246, 1961 (unpublished).

TABLE II. Beryllium data taken with incident electrons at $E_0=496.0\pm3.0$ MeV with a spectrometer momentum acceptance of $\Delta p/p=(2.203\pm0.003)\%$. The data cycle is given in column 1, the relative positron energy E/E_0 is given in column 2, and the background as a fraction of the empty-target rate B/R_0 is given in column 3. The target thickness at which pair and trident rates are equal t_{eq} is given in column 4 with the statistical errors in column 5. The (trident+quartet) rate T per radiation length per 10^5 electrons incident for $\Delta p/p=2.203\%$ is given in column 6 with the purely statistical errors ϵ_T(stat) in column 7. The error given in column 8 ϵ_T(net) is the statistical error combined quadratically with the error which would result from a 5% uncertainty in the background B. The (pair +triplet) rate P per (radiation length)^2 per 10^2 electrons incident for $\Delta p/p=2.203\%$ is given in column 9 with the corresponding statistical and net statistical-plus-background errors in columns 10 and 11.

1 Cycle	2 E/E_0	3 B/R_0	4 t_{eq} (in X_0)	5 ϵ_{eq}(stat) (%)	6 $T/(X_0)(10^5\ e^-)$ for $\Delta p/p=2.203\%$	7 ϵ_T(stat) (%)	8 ϵ_T(net) (%)	9 $P/(X_0^2)(10^2\ e^-)$ for $\Delta p/p=2.203\%$	10 ϵ_P(stat) (%)	11 ϵ_P(net) (%)
2	0.8009	0.72	0.00270	9.0	0.291	8.6	20.	0.218	2.3	3.1
6	0.8009	0.38	0.00329	8.2	0.351	7.9	8.9	0.215	2.4	2.5
2	0.9009	0.56	0.00289	6.4	0.129	6.3	10.7	0.0893	1.4	1.8
4	0.9009	0.38	0.00268	15.0	0.121	14.8	15.4	0.0905	2.2	2.2
6	0.9009	0.42	0.00230	8.5	0.106	8.4	9.8	0.0920	1.4	1.5
2	0.9508	0.51	0.00298	8.1	0.0367	7.8	10.5	0.0309	2.2	2.3
4	0.9508	0.39	0.00210	15	0.0326	14.8	15.4	0.0313	2.5	2.5
6	0.9508	0.50	0.00156	19	0.0250	19.1	20.4	0.0319	2.4	2.5
3	0.9819	0.40	0.00324	19	0.00698	18.2	18.7	0.00431	5.3	5.3
4	0.9819	−0.11	0.00438	21	0.00909	20.1	20.1	0.00416	6.5	6.5
5	1.0217	0.58	0.0509	462	0.00058	102	103	0.00002	451	451
6	1.0217	−0.32	−0.152	180	0.00106	48	48	−0.00001	173	173

The counting rate observed with the spectrometer set above E_0 (nominally at $1.02E_0$) was typically three orders of magnitude smaller than the rate at $0.80E_0$ for both tridents and pairs and for all three targets. If we assume that this rate was due entirely to photoprotons or electroprotons and use the calculated momentum dependence, we obtain an experimental limit of less than 0.5% for this background at $0.80E_0$ and less than 1% at $0.98E_0$. The similarity of the Čerenkov and scintillation counter rates also provided a limit of about 1% over most of the spectrum. We conclude, therefore, that this background was negligible.

The calculation of the trident rate T and pair rate P from the corrected data and the equations given in Appendix B was straightforward at most points, but there were two exceptions. First of all, measurements of the thick-target rate R_2 were made at $0.85E_0$ without the corresponding thin-target R_1 and empty-target R_0 determinations. We have obtained the necessary values for R_1 and R_0 by interpolating between the measurements of these quantities at $0.80E_0$ and $0.90E_0$, and we have used the interpolated values in calculating P at $0.85E_0$ for each element.

At $0.90E_0$ on cycle 2, the measured value of the empty-target rate R_0 was apparently incorrect. We have "adjusted" the common value of R_0 in this case to improve the agreement of the beryllium, aluminum, and platinum trident rates T from cycle 2 with the corresponding rates from the other cycles. In so doing, we have changed one measurement of R_0 in order to obtain better agreement of three otherwise independent results. The apparent error in R_0 may have been due to a fluctuation in the background, which was particularly large for this cycle (i.e., $B/R_0\sim0.5$ at $0.90E_0$ for cycle 2). If so, this is the only indication of such a fluctuation in the entire experiment.

As already mentioned, the thin-target R_1 and empty-target R_0 data were taken in a number of cycles down the recoil positron spectrum. This procedure was used as a precaution against possible fluctuations in the

TABLE III. Aluminum data taken with incident electrons at $E_0=497.0\pm3.0$ MeV with a spectrometer momentum acceptance of $\Delta p/p=(2.203\pm0.008)$ %. The column headings are the same as in Table II.

1 Cycle	2 E/E_0	3 B/R_0	4 t_{eq} (in X_0)	5 ϵ_{eq}(stat) (%)	6 $T/(X_0)(10^5\ e^-)$ for $\Delta p/p=2.203\%$	7 ϵ_T(stat) (%)	8 ϵ_T(net) (%)	9 $P/(X_0^2)(10^2\ e^-)$ for $\Delta p/p=2.203\%$	10 ϵ_P(stat) (%)	11 ϵ_P(net) (%)
2	0.8008	0.62	0.00380	5.6	0.449	5.1	11.1	0.234	2.5	2.9
5	0.8008	0.34	0.00320	9.6	0.386	9.3	9.9	0.241	2.6	2.6
6	0.8008	0.34	0.00324	6.7	0.391	6.3	7.1	0.242	2.2	2.2
2	0.9008	0.55	0.00266	7.1	0.137	6.8	10.5	0.103	2.0	2.2
4	0.9008	0.34	0.00257	10.7	0.133	10.5	11.1	0.104	2.2	2.2
5	0.9008	0.32	0.00253	10.1	0.131	9.9	10.4	0.104	2.1	2.1
2	0.9507	0.43	0.00229	7.4	0.0435	7.1	8.7	0.0379	2.1	2.2
3	0.9507	0.36	0.00274	13.9	0.0512	13.7	14.1	0.0374	2.5	2.6
4	0.9507	0.27	0.00207	13.1	0.0397	12.9	13.1	0.0383	2.3	2.3
5	0.9507	0.13	0.00253	10.8	0.0477	10.6	10.6	0.0377	2.3	2.3
3	0.9818	0.16	0.00319	14	0.0102	13.5	13.6	0.00638	4.0	4.1
5	0.9818	−0.007	0.00266	24	0.0086	23	23	0.00651	4.4	4.4
5	1.0216	0.08	−0.043	478	+0.0002	276	277	−0.00001	391	393

TABLE IV. Platinum data taken with incident electrons at $E_0=497.0\pm3.0$ MeV with a spectrometer momentum acceptance of $\Delta p/p=(2.203\pm0.008)$ %. The column headings are the same as in Table II.

1 Cycle	2 E/E_0	3 B/R_0	4 t_{eq} (in X_0)	5 ϵ_{eq}(stat) (%)	6 $T/(X_0)(10^5\ e^-)$ for $\Delta p/p=2.203\%$	7 ϵ_T(stat) (%)	8 ϵ_T(net) (%)	9 $P/(X_0^2)(10^2\ e^-)$ for $\Delta p/p=2.203\%$	10 ϵ_P(stat) (%)	11 ϵ_P(net) (%)
2	0.8007	0.58	0.00355	6.8	0.480	6.3	10.9	0.272	2.5	2.8
6	0.8007	0.24	0.00327	7.0	0.451	6.6	6.9	0.278	2.5	2.5
2	0.9007	0.46	0.00265	6.8	0.163	6.4	8.6	0.123	2.2	2.3
4	0.9007	0.15	0.00292	11.6	0.179	11.4	11.4	0.123	2.6	2.6
6	0.9007	0.13	0.00286	6.5	0.176	6.1	6.2	0.123	2.2	2.3
2	0.9506	0.23	0.00251	6.2	0.0597	5.8	6.2	0.0475	2.2	2.2
4	0.9506	0.32	0.00222	11.0	0.0536	10.8	10.8	0.0482	2.3	2.3
6	0.9506	0.07	0.00217	11.3	0.0524	11.1	11.1	0.0483	2.3	2.3
3	0.9817	−0.08	0.00229	17.0	0.0122	16	16	0.0106	4.0	4.0
6	0.9817	−0.39	0.00172	25	0.0094	25	25	0.0109	4.0	4.0
6	1.0215	0.54	−0.0316	198	0.0004	115	115	−0.00002	160	161

background, which contributed significantly to the R_1 and R_0 rates. The much higher thick-target rate R_1 was expected to be insensitive to fluctuations in the background, but the measurements at $0.80E_0$ were repeated for each element to verify within statistical errors of about 2% that this was true. The thick-target data at $0.80E_0$ were combined before the final calculations of the trident rate T and pair rate P were carried out.

The corrected data for the trident and pair rates are summarized in Tables II, III, and IV for beryllium, aluminum, and platinum, respectively. The cycle in column 1 refers to a particular measurement of R_0 and R_1 at the relative energy setting given in column 2. The incident energy is $E_1=497.0\pm3.0$ MeV. The ratio of the background to the empty-target rate, B/R_0, is given in column 3 of these tables. The background is obviously large, but the stability of B/R_0 *within each cycle* is encouraging. The differences in B/R_0 *for different cycles* and for different accelerator tuning provide a check that B can, in fact, be subtracted. We should mention that the estimated thickness of the ion chamber t_0 agreed with the bremsstrahlung measurement within 1%, so that the background, discussed in detail in Appendix B, certainly is not due to an error in t_0. The equivalent target thickness t_{eq} at which the trident and pair rates are equal is given in column 4 with the statistical errors in this quantity in column 5. The trident rate per radiation length per 10^5 electrons incident for $\Delta p/p=2.203\%$ is given in column 6 with the statistical error in column 7.

The statistical error in T is relatively large because of the large empty-target subtraction and the contamination of pairs, which is significant even for the $0.001X_0$ targets. For example, in the case of beryllium on cycle 2 at $0.90E_0$, the statistical errors were 1.2% in R_0, 0.9%

TABLE V. (Trident+quartet) and (pair+triplet) data from the different data cycles combined according to ϵ_T(net) and ϵ_P(net), respectively. The element is given in column 1 with the relative spectrum setting for tridents and for pairs in columns 2 and 3, respectively. These settings differ slightly with element and target thickness because of ionization energy losses. The combined (trident +quartet) and (pair+triplet) rates are given in columns 6 and 9 in the notation of Table II, and they are given again in columns 7 and 10 in μb per 2.203% and in (0.1 b)^2 for $\Delta p/p=2.203\%$, respectively. The final statistical-plus-background errors are given in columns 8 and 9. The systematic errors for T and for P are estimated in the text to be 2.3 and 2.2%, respectively.

1 Z	2 E/E_0 tridents	3 E/E_0 pairs	4 t_{eq} (in X_0)	5 ϵ_{eq}(stat) (%)	6 $T/(X_0)(10^5\ e^-)$ for $\Delta p/p=2.203\%$	7 T (barns) for $\Delta p/p=2.203\%$	8 ϵ_T(final) (%)	9 $P/(X_0^2)(10^2\ e^-)$ for $\Delta p/p=2.203\%$	10 P (0.1 b)^2 for $\Delta p/p=2.203\%$	11 ϵ_P(final) (%)
Be	0.8009	0.8033	0.00302	6.0	0.341	0.799	7.8	0.216	0.0119	2.0
Al	0.8008	0.8019	0.00352	3.9	0.402	7.53	5.1	0.240	0.843	2.0
Pt	0.8007	0.8009	0.00341	4.9	0.468	233	6.3	0.276	684	2.1
Be		0.8523						0.156	0.00856	2.5
Al		0.8509						0.173	0.607	2.3
Pt		0.8499						0.200	496	2.2
Be	0.9009	0.9033	0.00267	4.8	0.117	0.263	6.6	0.0908	0.00498	1.2
Al	0.9008	0.9019	0.00262	3.7	0.134	2.51	6.1	0.104	0.365	1.8
Pt	0.9007	0.9009	0.00278	4.3	0.173	86.1	4.6	0.123	305	1.9
Be	0.9508	0.9532	0.00214	6.6	0.0338	0.0762	7.5	0.0313	0.00172	2.0
Al	0.9507	0.9518	0.00238	5.2	0.0451	0.845	5.5	0.0379	0.133	1.7
Pt	0.9506	0.9508	0.00233	5.8	0.0571	28.4	4.8	0.0480	119	1.8
Be	0.9819	0.9843	0.00375	14	0.00804	0.0188	14	0.00427	0.000234	4.5
Al	0.9818	0.9829	0.00306	13	0.00987	0.185	13	0.00645	0.0266	3.6
Pt	0.9817	0.9819	0.00211	14	0.0114	5.67	14	0.0108	26.8	3.7
Be	1.0217	1.0241	−0.124	170	0.0009	0.00021	43	−0.000003	−0.0000002	150
Al	1.0216	1.0227	−0.043	478	0.0002	0.004	277	−0.00001	−0.00003	393
Pt	1.0215	1.0217	−0.032	198	0.0004	0.02	115	−0.00002	−0.05	161

TABLE VI. Systematic errors, in %.

	ϵ_M	ϵ_t	ϵ_{E_0}	$\epsilon_{\Delta p/p}$	ϵ_{TB}	ϵ_{MS}	ϵ_I	ϵ_{sys}
T	0.7	1.3	0.1	0.4	0.5	0.7	1.5	2.3
P	0.7	1.2	0.1	0.4	1.2	0.2	0.7	2.2

in R_1, and 0.8% in R_2. The statistical error propagated into T is 6.4%, while the statistical error in P is only 1.4%.

While the data from the different cycles are internally consistent (with the one exception mentioned above of R_0 at $0.90E_0$ on cycle 2), we feel that it would be inappropriate not to assign some error for the large background observed during the run. In column 8 of Tables II, III, and IV, we have given the net error ϵ_T(net) which would result from a 5% random uncertainty in the background, combined with the statistical errors in column 7. The importance of 5% fluctuations in the background can be judged for each point by comparing the errors in columns 7 and 8. The main effect of the additional background error is to reduce the statistical significance of those points, principally on cycle 2, where the background is large. The pair rates with the corresponding statistical and net background-plus-statistical errors are given in columns 9 and 10, and 11 of the tables.

In Table V, we have combined the trident results from the various cycles weighted according to ϵ_T(net) in column 8 of Tables II, III, and IV. The pair results, which depend essentially upon a single measurement of R_2 at each setting, have been weighted and combined according to $[\epsilon_P^2(\text{net})-\epsilon_{R_2}^2]^{1/2}$, where ϵ_{R_2} is the statistical error in R_2. The resulting error ϵ_P(final) is smaller than the separate errors ϵ_P(net) in Tables II, III, and IV, but larger than the errors which would result if the measurements of P were assumed to be completely independent.

Column 1 of Table V gives the element, while columns 2 and 3 give the respective energies for tridents and pairs relative to $E_0=497.0\pm3.0$ MeV. These energies differ slightly at each setting due to ionization losses. Column 4 gives t_{eq}, the thickness in radiation lengths at which the pair and trident rates are equal. The net statistical error in t_{eq} is given in column 5. The trident rate T per radiation length per 10^5 electrons incident for $\Delta p/p=2.203\%$ is given in column 6 and the cross section in μb per atom per 2.203% in column 7. The final "random" error in T, ϵ_T(final), is given in column 8. The pair rate per (radiation length)^2 per 10^2 electrons incident for $\Delta p/p=2.203\%$ is given in column 9, and the product of the bremsstrahlung and pair cross sections in (0.1 b)^2 for $\Delta p/p=2.203\%$ is given in column 10 with the final "random" error in column 11.

For simplicity we are estimating typical values for the systematic errors other than those associated with the background. As mentioned earlier, the absolute uncertainty ϵ_M in monitoring the beam is $\pm0.7\%$, while the errors in making counting rate corrections are negligible. The uncertainties in target thickness are propagated into the experimental values of T and P by the approximate expressions:

$$\epsilon_t(T)\equiv\frac{dT}{T}=\left[\left(0.7\frac{dt_0}{t_0}\right)^2+\left(2.3\frac{dt_1}{t_1}\right)^2+\left(2.0\frac{dt_2}{t_2}\right)^2\right]^{1/2}, \quad (10a)$$

$$\epsilon_t(P)\equiv\frac{dP}{P}=\left[\left(0.4\frac{dt_1}{t_1}\right)^2+\left(2.9\frac{dt_2}{t_2}\right)^2\right]^{1/2}. \quad (10b)$$

Assuming $dt_0/t_0=0.5\%$, $dt_1/t_1=0.4\%$, and $dt_2/t_2=0.4\%$, we obtain $\epsilon_t(T)=1.3\%$ and $\epsilon_t(P)=\pm1.2\%$.

The trident and pair rates at 500 MeV are relatively insensitive to E_0 for a given $\Delta p/p$ and a given value of E/E_0:

$$\epsilon_{E_0}(T)=\frac{dT}{T}<0.1\frac{dE}{E}, \quad (11a)$$

$$\epsilon_{E_0}(P)=\frac{dP}{P}\sim0.3\frac{dE}{E}. \quad (11b)$$

The corresponding systematic errors are less than 0.2%, which is negligible. The uncertainty in $\Delta p/p$ is propagated linearly into the trident and pair rates and amounts to $\pm0.4\%$ as determined by BGY. The spectrometer field was reversible for positrons and electrons to $\pm0.1\%$ so that the absolute uncertainty in E/E_0 is of this order when both E and E_0 are derived from the spectrometer settings. The relative uncertainty of different settings on the same spectrum is about $\pm0.03\%$, as found by BGY.

The error associated with the correction for bremsstrahlung losses in the targets is about 10% of the net correction, diluted somewhat by the relative importance of the (R_1-R_0) and (R_2-R_0) terms in the expressions for T and P. The results are $\pm1.2\%$ or less for $\epsilon_{TB}(P)$ and $\pm0.5\%$ or less for $\epsilon_{TB}(T)$. The uncertainties in the Landau straggling losses are $\pm0.2\%$ or less and can be neglected. The multiple-scattering uncertainties are $\epsilon_{MS}(T)=\pm0.7\%$ and $\epsilon_{MS}(P)=\pm0.2\%$, as already discussed.

The only correction which is quite different for different Z and different E/E_0 is that due to ionization in targets having quite different thicknesses in g/cm^2. An error assignment of $\epsilon_I(T)=\pm1.5\%$ and $\epsilon_I(P)=\pm0.7\%$ is conservative for all targets and all momentum settings except beryllium at $0.95E_0$ and $0.98E_0$ and aluminum at $0.98E_0$. Since the statistical errors are large for points near E_0, the values chosen for ϵ_I at $0.98E_0$ are of little importance. The main systematic errors in the experiment are summarized below in Table VI.

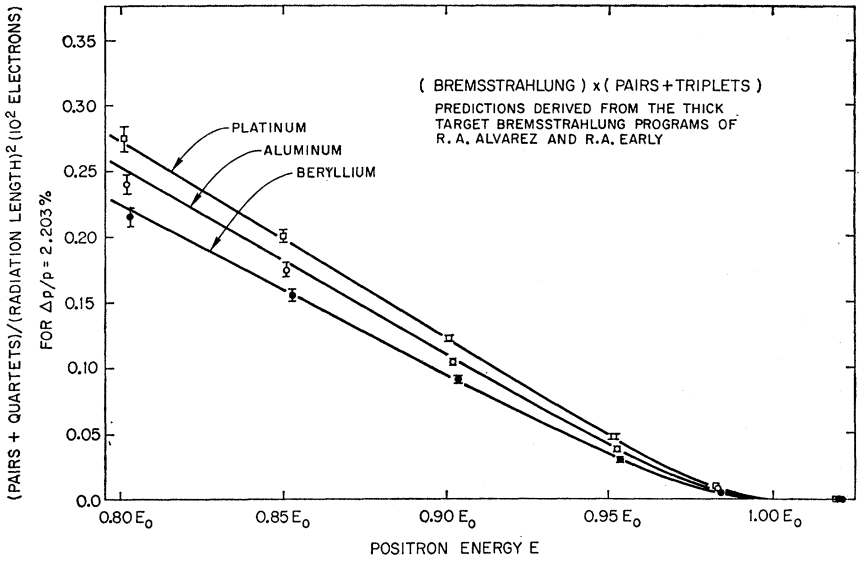

FIG. 6. Experimental (pair +triplet) spectra for beryllium, aluminum, and platinum plotted with the predictions obtained by folding together the bremsstrahlung program of Alvarez and of Early and the pair-production program derived from it. These programs contain detailed calculations of the screening effects, and they take into account electron-electron bremsstrahlung as well as triplet production.

V. DISCUSSION

There are several points which should be clarified before we compare the pair and trident data with various theoretical predictions. First of all, we have made no radiative corrections either to the data or to the theoretical predictions. The real and virtual radiative corrections to the bremsstrahlung and pair-production spectra have been calculated by Mork and Olsen,[33] and combined they amount to less than 2% except quite near the incident energy E_0. This is comparable with the systematic errors in the pair production case as well as with the other theoretical uncertainties anticipated in the product of the computed bremsstrahlung and pair-production cross sections. The radiative corrections to the trident cross section[34] are even smaller than those for bremsstrahlung or pair production, and they can be neglected.

As mentioned in the previous section, there is an uncertainty of order $\pm 0.1\%$ in the absolute setting of E/E_0, related to the reversibility of the spectrometer for positrons and electrons. Within these narrow limits, the pair and trident data points can be shifted *together* relative to the theoretical spectra. (In principle, points could be shifted relative to each other by $\pm 0.03\%$, but this has negligible effect over most of the spectrum.)

The threshold for producing pairs or tridents is $2mc^2$.[35] This is taken into account in the lower limit of the integration over the intermediate photon energy k. A "cutoff" is used at the upper limit to prevent divergences. To be specific, the lower and upper limits are $E+2mc^2$ and $0.999E_0$, respectively, for all calculations which follow.

We have said very little so far about screening. Screening becomes effective when the minimum momentum transfer $q_{\min}$ is less than the reciprocal atomic radius. In the notation of MUT we have for tridents

$$q_{\min}=\frac{km^2(1+x^2)}{2E_+E_-}\ll\frac{mZ^{1/3}}{137}, \tag{12}$$

for complete screening. Screening is not effective when the momentum transfer is much greater than the reciprocal atomic radius, i.e., when the inequality in Eq. (12) is reversed. These conditions are, of course, equivalent to statements that one or the other of the two screening functions given, respectively, for L or for L' should dominate; the correct expression is the smaller of the two. For our experimental conditions, screening effects are expected to be less than 2%.[34] Similar expressions hold for bremsstrahlung and pair production, but the question is resolved formally in the thick-target bremsstrahlung program and in the pair-production program derived from it; for $Z>1$, the Fermi-Thomas model is used.

In Fig. 6 we have plotted the (pair+triplet) data with the predictions obtained by folding together the bremsstrahlung and pair-production cross sections of Eqs. (4a)–(4h) and (5a). The data have not been shifted relative to the theoretical curves since the agreement is already satisfactory. In particular, the χ^2 probability for the twelve points (and eleven degrees of freedom) in the range $0.80E_0$ to $0.95E_0$ is 0.90 when the combined systematic ($\sim 2\%$) and statistical ($\sim 2\%$) errors are used. The χ^2 probability for the purely statistical errors is 0.34.

The beryllium, aluminum, and platinum points at $0.98E_0$ differ from the predicted rates by about -12, -10, and $+17\%$, respectively. These differences are much larger than the systematic and statistical errors

[33] K. Mork and H. Olsen, Phys. Rev. **140**, B1661 (1965).
[34] S. Brodsky (private communication).
[35] The threshold for triplets and quartets is $4\,mc^2$, or twice that for pairs and tridents. The distinction is not very important here since the nuclear processes dominate.

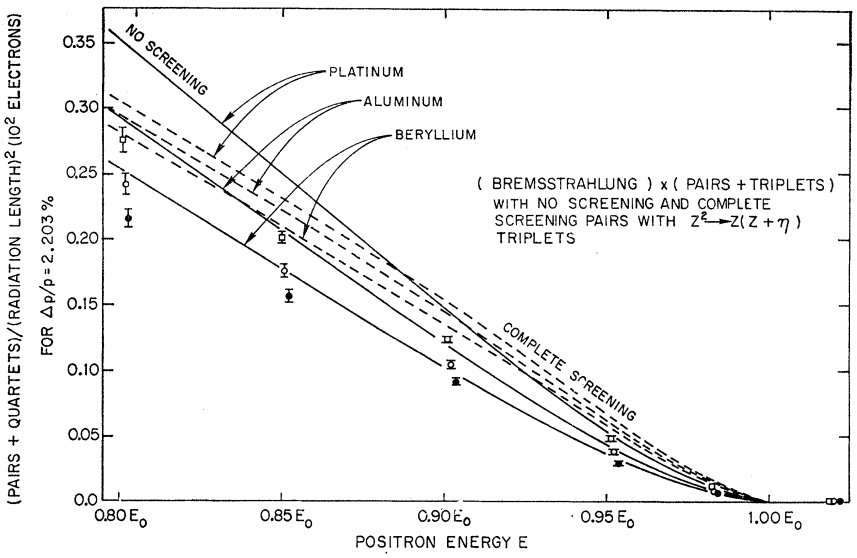

FIG. 7. Experimental (pair +triplet) spectra for beryllium, aluminum, and platinum plotted with the predictions obtained by folding together the bremsstrahlung program of Alvarez and of Early and a pair production program for the Bethe-Heitler formula. Triplet production has been taken into account by the substitution $Z^2 \rightarrow Z(Z+\eta)$, where η is the ratio of the total cross sections for electron-electron and electron-nucleon bremsstrahlung.

given explicitly in Table III and in Table V, but they can be explained by the observation that at this setting, a 0.03% change in E/E_0 results in a 10% change in the predicted cross sections. At $0.95E_0$ the corresponding change is only 1% so that the twelve points used in calculating the χ^2 probability are essentially free of this effect.

The absolute agreement of the (pair+triplet) data with the theoretical predictions on the 2–3% level is really quite remarkable. Within these errors, the dependence of the bremsstrahlung and pair-production cross sections upon E/E_0 and upon Z is verified. It is clear, for example, that both electron-electron bremsstrahlung and triplet production are effective. Roughly speaking, they enhance the product of the two cross sections by

$$(Z+\eta)^2/Z^2 \approx 1.748 \quad \text{for Be} \qquad (13a)$$

$$\approx 1.199 \quad \text{for Al} \qquad (13b)$$

$$\approx 1.030 \quad \text{for Pt}, \qquad (13c)$$

where η is calculated from the equations given in Appendix A. Thus our 3% experimental uncertainty can be interpreted as a 7% uncertainty in the net electron-electron bremsstrahlung and triplet-production contributions to the double cross section for beryllium. Barring fortuitous cancellations, the processes involving atomic electrons have been individually verified to an accuracy of about 15% for beryllium. The platinum results indicate that the purely nuclear contributions are predicted correctly to 3% in the range

$$0.80E_0 \leq E \leq 0.95E_0.$$

In Fig. 7 we have plotted the (pair+triplet) data with the predictions derived by folding together the bremsstrahlung cross section of Eqs. (4a)–(4h) with the no-screening and complete-screening pair-production cross sections of Eqs. (5b)–(5c). Triplet production has been taken into account by the approximate substitution $Z^2 \rightarrow Z(Z+\eta)$. Since the bremsstrahlung part of the calculation has already been tested and verified in Fig. 6, this is primarily a test of the pair-production formula with some ambiguity for the low-Z elements where η is significant. Among other things, this comparison illustrates that the data are able to distinguish between various theoretical calculations and that the agreement obtained in Fig. 6 is not a trivial consequence of the roughly linear energy dependence which results from the integration over k or of the simple Z dependence of the radiation length unit.

In comparing the (trident+quartet) data with the predictions of Bhabha and of MUT, we should note first of all that the settings in E/E_0 have already been fixed by the more precise (pair+triplet) results. Only the two constants $C_1 \sim C_2 \sim 1$ for the Bhabha trident cross section and the single constant $C_3 \sim 1$ for the MUT cross section remain as free parameters, presumably to be determined by experiment. We shall arbitrarily set C_2 equal to unity since the Bhabha cross section is far more sensitive to C_1 than to C_2. In addition, we shall take quartets into account by the usual substitution $Z^2 \rightarrow Z(Z+\eta)$.

The (trident+quartet) data are plotted in Fig. 8 with the predictions of Bhabha, i.e., of the Weizsäcker-Williams approximation. The complete-screening calculations expressed in radiation length units show very little Z dependence, and a reasonable fit is not possible in this case. For $C_2 \equiv 1$ in Eqs. (1a)–(1d), the best fit for the no-screening curves is obtained with

$$C_1 = 1.14 \pm 0.01. \qquad (14)$$

The χ^2 probability for the nine points (and eight degrees of freedom) at nominal positron energies of $0.80E_0$, $0.90E_0$, and $0.95E_0$ is about 0.01. The points at

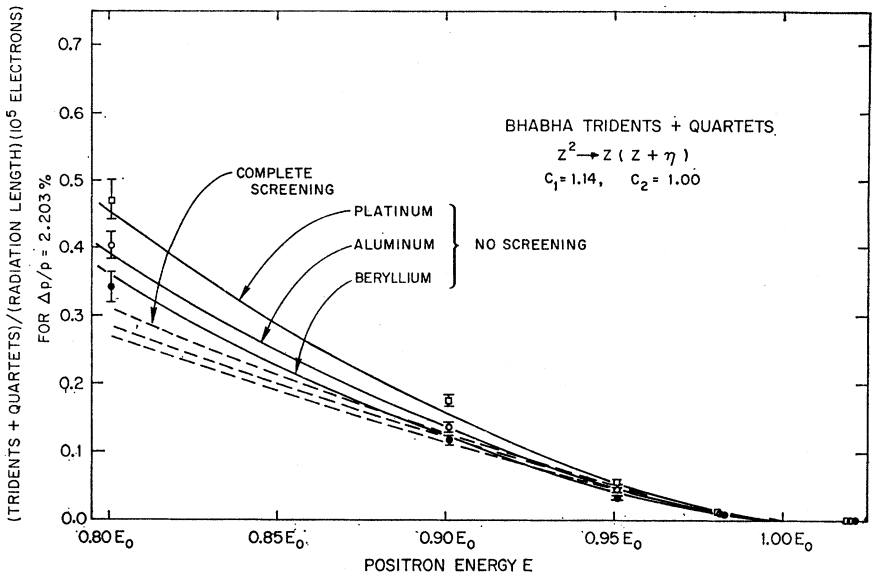

FIG. 8. Experimental (trident +quartet) spectra for beryllium, aluminum, and platinum plotted with the predictions of Bhabha and of the Weizsäcker-Williams approximation. Quartet production has been taken into account by the substitution $Z^2 \rightarrow Z(Z+\eta)$, where η is the ratio of the total cross sections for electron-electron and electron-nucleon bremsstrahlung. For $C_2 \equiv 1.00$, the best fit for the no-screening curves is obtained with $C_1 = 1.14 \pm 0.01$, which yields a χ^2 probability of about 0.01.

$0.98E_0$ fall several standard deviations below the Bhabha predictions. While the Weizsäcker-Williams approximation does not appear to give an adequate fit to our data, it does agree qualitatively and would give a reasonable χ^2 probability if an additional "theoretical error" were assumed comparable with the ~6% experimental errors at each point.

The experiment of Camac on copper at $E_0 = 230 \pm 30$ MeV and at $E/E_0 = 0.80$ yielded a value of $C_1 = 1.6 \pm 0.2$, which is clearly different from the present result. To be more explicit, the ratio of the Bhabha cross sections at $0.80E_0$ and 500 MeV for the two values of C_1 is

$$\sigma_{\text{Bhabha}}(C_1 = 1.6 \pm 0.2)/\sigma_{\text{Bhabha}}(C_1 = 1.14 \pm 0.01) = 2.4 \pm 0.6. \quad (15)$$

This discrepancy is not a question of screening since the no-screening case seems still to be applicable at 500 MeV and would certainly be applicable at 230 MeV. It is not a question of the Z dependence since this is small and fairly well described by the no-screening equation. Finally, it is not a question of a possible energy dependence of the "constant" C_1 since the ratios of the Bhabha and MUT cross sections are similar at 230 and 500 MeV when the same values of C_1, C_2, and C_3 are used.

As noted by BGY, the MUT equations with complete screening correspond to a value of $C_1 \approx 1.35$, which is not inconsistent with the Camac result of $C_1 = 1.6 \pm 0.2$. However, since the no-screening case seems to be applicable and since the no-screening predictions of MUT are rather smaller than the complete-screening results, the discrepancy between Bhabha ($C_1 = 1.6 \pm 0.2$)

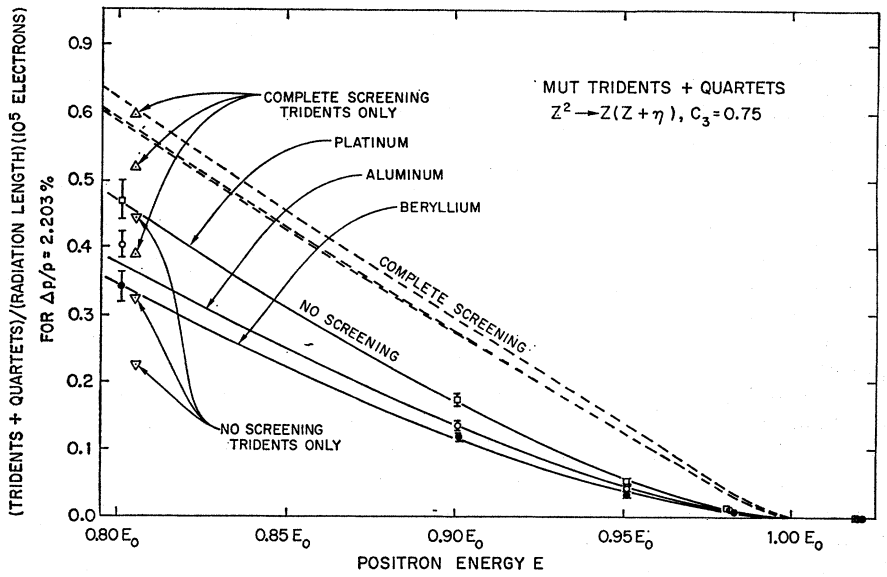

FIG. 9. Experimental (trident +quartet) spectra for beryllium, aluminum, and platinum plotted with the predictions of MUT. Quartet production has been taken into account by the usual substitution $Z^2 \rightarrow Z \times (Z+\eta)$. The best fit for the no-screening curves is obtained with $C_3 = 0.75 \pm 0.05$, which yields a χ^2 probability of 0.22.

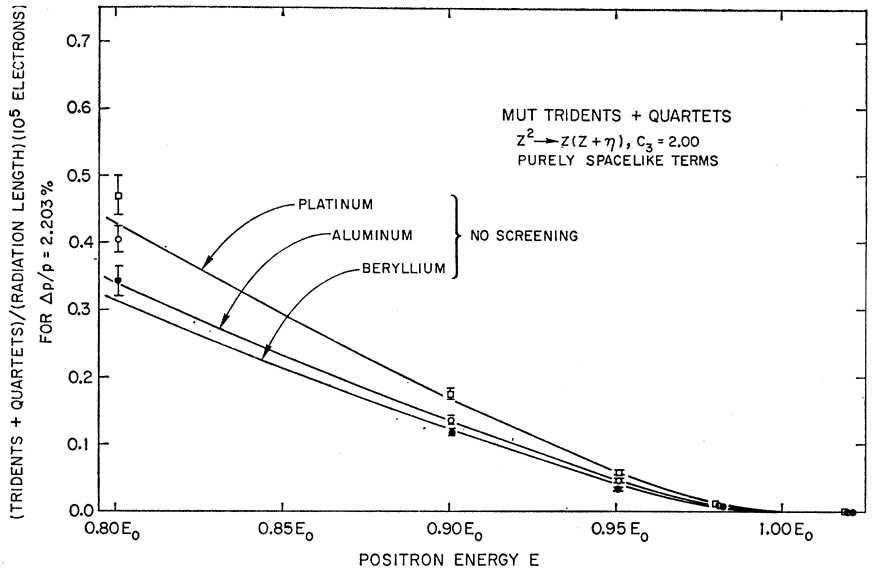

FIG. 10. Experimental (trident+quartet) spectra for beryllium, aluminum, and platinum plotted with the purely spacelike predictions of MUT. Quartet production has been taken into account by the usual substitution $Z^2 \rightarrow Z(Z+\eta)$. The best fit for the no-screening curves is obtained with $C_3 = 2.00 \pm 0.20$, which yields a χ^2 probability of much less than 0.01.

and MUT is large and comparable with the experimental discrepancy of Eq. (15). As already mentioned, the trident background for BGY was only of order 1% so that the error made by using MUT with complete screening or Bhabha with $C_1 \approx 1.35$ was typically 0.5% in that experiment. This is about half the assigned error for the most precise BGY points.

The (trident+quartet) data are plotted in Fig. 9 with the no-screening and complete-screening predictions of MUT. The parameter C_3 has a value

$$C_3 = 0.75 \pm 0.05, \tag{16}$$

and the χ^2 probability for the nine points (and eight degrees of freedom at nominal energies of $0.80E_0$, $0.90E_0$, and $0.95E_0$) is 0.22 for the no-screening case. Since $d\sigma_{\mathrm{MUT}}/\sigma_{\mathrm{MUT}} \sim 0.5 dC_3/C_3$, the MUT cross sections with $C_3 \equiv 1$ are only about 12% higher than the experiment or about twice the 6% experimental errors on a typical point. The differences between experiment and theory at $0.98E_0$ are $+22$, $+33$, and -7% for beryllium, aluminum, and platinum, respectively. These differences are reasonably compatible with the ~ 15% statistical errors at these points combined with the ~ 10% error associated with the ± 0.03% relative uncertainty in E/E_0.

As in the case of the Bhabha (trident+quartet) predictions, a reasonable fit with the complete-screening curves of MUT cannot be obtained by a suitable choice of the available parameters; nor is a satisfactory fit possible which excludes quartets. In this sense, the 6% experimental accuracy is equivalent in the case of beryllium to a ~ 25% measurement of the quartet cross section. Finally, we have tried in Fig. 10 to fit the data with the purely spacelike cross section of MUT and have found that a value $C_3 = 2.0 \pm 0.20$ is about optimum. The χ^2 probability is, however, much less than 0.01, indicating that the timelike terms are necessary.

We may summarize the results of this experiment by noting that the (pair+triplet) spectra for beryllium, aluminum, and platinum agree with the theoretical predictions within typical experimental errors of 3% (Fig. 6). The corresponding (trident+quartet) spectra agree with the no-screening predictions of MUT (Fig. 9) within typical experimental errors of 6% when the MUT constant has the value $C_3 = 0.75 \pm 0.05$ and when the contributions of the atomic electrons are taken into account by the substitition $Z^2 \rightarrow Z(Z+\eta)$. A satisfactory fit cannot be obtained if complete screening is assumed or if the electron contributions are left out; nor is a satisfactory fit possible with the purely spacelike cross section. While the MUT calculation is uncertain due to the neglect of both the exchange and the interference terms, it nevertheless provides an excellent parametrization of our (trident+quartet) results.

ACKNOWLEDGMENTS

This experiment could not have been carried out without the support and assistance of many people both at the Orsay Linear Accelerator Laboratory and at the Stanford Linear Accelerator Center. In particular, we would like to acknowledge the generous support of Professor A. Blanc-Lapierre of LAL and of Professor R. Mozley of SLAC. Dr. S. Brodsky of SLAC contributed many useful discussions. The preparation and analysis of the targets was handled by W. Schultz at SLAC. The successful completion of the data run during a limited period of time was assured by the complete cooperation of Dr. B. Milman, Dr. L. Burnod, and the entire staff and crew of the Orsay Linear Accelerator Laboratory.

APPENDIX A: TARGET-THICKNESS DATA

The target thicknesses obtained from the weights and the areas of each sample are summarized in Table

TABLE VII. Target thicknesses determined from the weight per unit area.

1	2	3	4	5	6	7	8	9	10	11
Z	g/cm²	$\pm\epsilon$%	δ_{TI} (%)	$\pm\epsilon_{TI}$ (%)	Final g/cm²	g/cm²/X_0	t in X_0	Atoms/cm² (10^{22})	Electrons/cm² (10^{22})	$\pm\epsilon_{final}$ (%)
4(Be)	0.07332	±0.3	+0.0	±0.0	0.07332	63.87	0.001148	0.4900	1.960	±0.3
4(Be)	1.2414	±0.1	+0.0	±0.0	1.2414	63.87	0.01944	8.296	33.18	±0.1
13(Al)	0.02625	±0.3	+0.9	±0.2	0.02649	23.90	0.001108	0.05915	0.7690	±0.4
13(Al)	0.5452	±0.1	+1.8	±0.2	0.5550	23.90	0.02322	1.239	16.11	±0.3
78(Pt)	0.00733	±0.4	+0.0	±0.0	0.00733	6.505	0.001127	0.002264	0.1766	±0.4
78(Pt)	0.1294	±0.4	+0.0	±0.0	0.1294	6.505	0.01989	0.03996	3.117	±0.4

VII. The first column gives the element while the second and third give the thickness in g/cm² and the uncertainties in these measurements. A small correction for the target impurities determined by spectroscopic analysis[36] is given with associated errors in the next two columns. This correction to the thickness in radiation lengths is significant only for aluminum and is given by

$$\delta_{TI}=\sum \Delta_{TI},$$
$$\Delta_{TI}=f_I\left[\frac{Z_I^2}{Z_0^2}-\frac{A_I}{A_0}\right], \quad \text{(A1)}$$

where f_I is the fraction of the target atoms of a given impurity, Z_I is the atomic number, and A_I is the atomic weight of these atoms, and Z_0 and A_0 are the atomic number and atomic weight of the principal constituent. The corrected thickness in g/cm² is given for each target in column 6 of Table VII.

In determining the target thicknesses in radiation lengths, we have used the definition of the radiation length contained in the thick-target bremsstrahlung program.[24–26] The radiation length in g/cm² is given by

$$1/X_0=(4\alpha N r_e^2/A)Z(Z+\eta)\ln(183/Z^{1/3}), \quad \text{(A2a)}$$

where α is the fine-structure constant, N is Avogadro's number, A is the atomic weight, r_e is the classical electron radius, and Z is the atomic number. The function η, which is due to the atomic electrons and which is the ratio of the total cross sections for electron-electron and electron-nucleon bremsstrahlung, is given for $Z>1$ by the expression

$$\eta=\frac{28.4-(8/3)\ln Z}{20.94-(4/3)\ln Z-4f(Z)}, \quad \text{(A2b)}$$

where $f(Z)$ is the Coulomb correction term given in Eqs. (4d) and (4c) of the text.

The calculated radiation length in g/cm² is given for each element in column 7 of Table VII. The thickness of each target in radiation lengths is given in column 8, the number of atoms/cm² in column 9, the number of electrons/cm² in column 10, and the estimated uncertainties in these quantities in the final column, column 11.

The uncorrected ratios of the thin/thick target thicknesses obtained for each element in the bremsstrahlung transmission experiment are given in column 2 of Table IX. To first order, the number of electrons in the tail of the energy distribution is proportional to the target thickness in radiation lengths, but second-order corrections must be made for the depletion of electrons out of the incident spectrum.

The effect of hard-photon emission upon the electron energy spectrum is calculated in the thick-target bremsstrahlung program using the formula of Eyges.[37] The probability $P(E_0, E, t)$ of finding an electron of original energy E_0 whose energy lies between E and $E+dE$ at a distance t radiation lengths into the target is given by

$$P(E_0,E,t)dE=(1+a)^{Bt}(E/E_0)^a \times\frac{[\ln(E_0/E)]^{Bt-1}}{\Gamma(Bt)}\frac{dE}{E_0}, \quad \text{(A3)}$$

where $B=kn(k)$ for a photon energy $k=0$ (approximately $\frac{4}{3}$) and where $a=0.25$ for this program.

The first correction δ_{TTB} applied to the experimental bremsstrahlung ratios is defined to be the difference in percent in the ratios computed from Eq. (A3) at a given point on the tail of the electron spectrum and the ratios of the target thicknesses assumed in the computation. These corrections to the thin/thick$=t_1/t_2$ ratios are negative due to the net loss of electrons in the thick-target t_2 case.

The formula of Eyges, Eq. (A3), does not include corrections for the shifting of the electron spectrum due to ionization or for the enhancement associated with Landau straggling. The ionization correction for a given target is just

$$\delta_I=\frac{\Delta E_I}{k}=\frac{\Delta E_I}{E_0-E}, \quad \text{(A4)}$$

where ΔE_I is the energy loss due to ionization in the target and $k=E_0-E$ is the difference in incident and final electron energies. The total energy loss when a

[36] The spectroscopic analysis was carried out by Western Gold and Platinum Co., Spectrograph Lab, 525 Harbor Blvd., Belmont, Calif.

[37] L. Eyges, Phys. Rev. **76**, 264 (1949).

TABLE VIII. Ionization energy loss.

Target	t_0	$0.001X_0$ Be	$0.020X_0$ Be	$0.001X_0$ Al	$0.020X_0$ Al	$0.001X_0$ Pt	$0.02X_0$ Pt
ΔE_I (MeV)	0.036	0.156	2.03	0.081	0.958	0.045	0.203

particular target is in the beam is given in Table VIII, and the ionization corrections are given in column 4 of Table IX.

In first order, Landau straggling is similar to bremsstrahlung in that it adds to the tail of the electron distribution a term linear in target thickness[38]:

$$L(\epsilon)d\epsilon=\frac{0.15Z}{A}l\frac{d\epsilon}{\epsilon^2}, \tag{A5}$$

where l is the target length in g/cm^2 and where $\epsilon=E_0-E$ is expressed in MeV. The Landau process differs from bremsstrahlung in its Z dependence (Z versus Z^2) and in its energy dependence (dE/E^2 versus dk/k). The Landau correction to the target-thickness data δ_L in column 5 of Table IX, is analogous to, but much smaller than the "thick-target bremsstrahlung correction" δ_{TTB}. Furthermore, due to the more rapid energy dependence in the Landau case, there is a net enhancement in second order ("scattering-in exceeds scattering-out") instead of the reverse. Thus the Landau correction to t_1/t_2 is positive.

The net corrections to the raw target-thickness data are given in column 6 of Table IX. The corrected ratios are given in column 7. The ratios of the thicknesses in Table VII are given in column 8, and the differences Δ in the ratios determined by the two methods are given in column 9. The statistical uncertainties in the bremsstrahlung ratios, which are in the range ±0.5 to $\pm1.0\%$, have been combined with the less than $\pm0.6\%$ uncertainties in the ratios computed from Table VII and with an assumed systematic uncertainty of $\pm10\%$ of the tabulated corrections of Table IX to get the final error $\pm\epsilon_{\text{final}}$ in column 10 of Table IX.

Looking now at Table IX we observe that the differences in the target-thickness ratios are consistent with zero within the assigned errors, which range from ±1 to $\pm2\%$. More precisely, the mean value of Δ is $(+0.3\pm0.7)\%$, and the standard deviation for a single measurement is $\pm1.7\%$. The agreement of the values at different settings on the electron spectrum (nominally at $E=0.96E_0$ and at $E=0.92E_0$) provides an excellent check of the corrections in Table IX, while the over-all consistency of the data severely limits any possibility of target nonuniformity. This is particularly helpful in the case of platinum where the corrections and errors in the bremsstrahlung data are smallest and where the question of target uniformity is most seriously raised.

The thickness t_0 of the ion chamber beam intensity and position monitors was determined separately as part of the bremsstrahlung data for each element. The results averaged at $0.96E_0$ and at $0.92E_0$ were $(0.941\pm0.010)\times10^{-3}X_0$ relative to the thin beryllium, $(0.925\pm0.020)\times10^{-3}X_0$ relative to the thick beryllium, $(0.913\pm0.010)\times10^{-3}X_0$ relative to the thin aluminum, $(0.934\pm0.015)\times10^{-3}X_0$ relative to the thick aluminum, $(0.912\pm0.010)\times10^{-3}X_0$ relative to the thin platinum, and $(0.915\pm0.010)\times10^{-3}X_0$ relative to the thick platinum. The average of these measurements is $(0.923\pm0.005)\times10^{-3}X_0$. The value estimated from the aluminum foil thicknesses of BGY and from the smaller thicknesses of the Mylar windows and hydrogen gas is $(0.915\pm0.006)\times10^{-3}X_0$. The difference in the two values is $(0.008\pm0.008)\times10^{-3}X_0$.

Two additional observations concerning the bremsstrahlung data will be of interest in Appendix B. First of all, the "empty" target data place a limit upon the product of the fraction f of the primary beam which passes through any spurious target material and the thickness of this material t_s

$$ft_s<1\%. \tag{A6}$$

Secondly, the ratios of the target thicknesses for the different elements provide a sensitive test of the radiation length unit X_0 if Eqs. (A2a) and (A2b) for the case of low-energy bremsstrahlung. This test is summarized in Table X where the ratios of the corresponding target

TABLE IX. Bremsstrahlung and weight/area target-thickness ratios (same element, different thickness).

1 $Z(E/E_0)$	2 t_1/t_1 raw	3 δ_{TTB} (%)	4 δ_I (%)	5 δ_L (%)	6 δ_{NET} (%)	7 t_1/t_2 final	8 t_1/t_2 Table VII	9 Δ (%)	10 $\pm\epsilon_{\text{final}}$ (%)
Be(0.96)	0.05491	−5.4	+9.5	+1.3	+4.9	0.05764	0.05906	−2.4	±2.0
Be(0.92)	0.05811	−3.7	+4.4	+0.1	+0.6	0.05846		−1.0	±2.0
Al(0.96)	0.05022	−6.5	+3.7	+0.2	−2.9	0.04876	0.04773	+2.1	±1.5
Al(0.92)	0.05030	−4.4	+1.8	+0.0	−2.7	0.04894		+2.5	±1.5
Pt(0.96)	0.06052	−6.5	+0.9	+0.0	−5.7	0.05706	0.05665	+0.7	±1.0
Pt(0.92)	0.05898	−4.4	+0.5	+0.0	−4.1	0.05655		−0.2	±1.0

[38] D. M. Ritson, *Techniques of High Energy Physics* (Interscience Publishers, Inc., New York, 1961).

TABLE X. Bremsstrahlung and weight/area target-thickness ratios (same thickness, different element).

1 $Z(E)/Z(E)$	2 t_1/t_1 Brem.	3 t_2/t_2 Brem.	4 t_0/t_1 X_0	5 t_2/t_2 X_0	6 Δ_1 (%)	7 Δ_2 (%)	8 $\bar{\Delta}_1$ (%)	9 $\bar{\Delta}_2$ (%)	10 Δ (%)
Be(0.96)/Al(0.96)	1.012	0.856	1.036	0.837	−2.4	+2.3	−3.3	+0.9	−1.2
Be(0.92)/Al(0.92)	0.995	0.833			−4.1	−0.5			
Be(0.96)/Pt(0.96)	0.986	0.976	1.019	0.977	−3.3	−0.1	−3.3	−1.1	−2.2
Be(0.92)/Pt(0.92)	0.987	0.955			−3.2	−2.2			
Al(0.96)/Pt(0.96)	0.974	1.140	0.983	1.167	−0.9	−2.3	+0.0	−2.0	−1.0
Al(0.92)/Pt(0.92)	0.992	1.147			+0.9	−1.7			

thicknesses with different Z are given. The ratios are identified in column 1 of Table X, the corrected ratios from the bremsstrahlung tail are given for the thin and thick targets in columns 2 and 3, and the ratios calculated from the weights and areas and from the radiation length unit are given in columns 4 and 5. In columns 6 and 7 the differences in the bremsstrahlung tail and the calculated values are given. The differences at $0.96E_0$ and $0.92E_0$ are combined in columns 8 and 9, and the thin- and thick-target results are combined in column 10. The estimated errors are about $\pm 2\%$ for the ratios involving beryllium and about $\pm 1.5\%$ for aluminum/platinum. The data are reasonably consistent within these errors, and they indicate that the Z dependence of low-energy bremsstrahlung is factored out in the radiation length unit to about $\pm 2\%$ from $Z=4$ to $Z=78$. The absolute magnitude of the bremsstrahlung tail has been measured by BGY for CH_2, Al, and Be in our region; the results agree with the predictions of Eqs. (4a)–(4h) within experimental errors of about 5%.

APPENDIX B: EXTRACTION OF T, P, AND B

We will first consider the separation of the direct (triplet+quartet) process from the cascade (pair +triplet) process. Let T be the event rate per unit target thickness per unit momentum interval for the first process and P be the event rate per unit target thickness squared per unit momentum interval for the second. Clearly P is the product of the separate bremsstrahlung and pair rates. In addition, we will begin by assuming a background B which is the same for any target and which can therefore be subtracted out by means of an "empty-target" measurement.

In this experiment, the minimum target t_0 consists of an ion chamber, which remains always in the electron beam. We will let t_1 be the thin $(0.001X_0)$ target of a given element and t_2 be the thick $(0.02X_0)$ target. The experimental rates are then

$$R_0=B+t_0T+\tfrac{1}{2}t_0^2P, \tag{B1a}$$

$$R_1=B+(t_0+t_1)T+\tfrac{1}{2}(t_0+t_1)^2P, \tag{B1b}$$

$$R_2=B+(t_0+t_2)T+\tfrac{1}{2}(t_0+t_2)^2P. \tag{B1c}$$

These equations can be solved for T, P, and B exactly and yield

$$T=\left(\frac{R_1-R_0}{t_1}\right)\left(\frac{t_2+2t_0}{t_2-t_1}\right)-\left(\frac{R_2-R_0}{t_2}\right)\left(\frac{t_1+2t_0}{t_2-t_1}\right), \tag{B2a}$$

$$P=\frac{2}{(t_2-t_1)}\left[\frac{(R_2-R_0)}{t_2}-\frac{(R_1-R_0)}{t_1}\right], \tag{B2b}$$

$$B=R_0-\frac{t_0}{(t_2-t_1)}\left[(R_1-R_0)\frac{(t_2+t_0)}{t_1}-(R_2-R_0)\frac{(t_1+t_0)}{t_2}\right]. \tag{B2c}$$

The background B is subtractable in the sense that the expressions for T and P involve only the target thicknesses and the differences in the experimental rates, specifically (R_1-R_0) and (R_2-R_0). However, the form initially assumed for B is only a special case and may or may not correspond to the experimental situation. Since B is experimentally large, it is important to try to determine its origin.

On the basis of preliminary runs with no material in the beam, we can say that the background due to spurious positrons in the beam or to the beam stopping in the magnet iron is about 2% of the counting rate for the thin targets. This is of the order of two counts per 10^{11} electrons incident. Since even the thick target is thin from the point of view of multiple scattering, these relatively small contributions are of the subtractable form assumed. A third source that must concern us is the target holder, which was quite similar, but not identical for each target used. A comparison of the empty-target rates R_0 with and without an empty target holder in the beam gave an enhancement of $(1.4\pm 1.4)\%$. While this background may be less reproducible than those due to positrons in the electron beam or to the beam stopping in the spectrometer, it too is quite small and is, in fact, statistically consistent with zero.

Let us now consider the background which would result from a small fraction of the beam hitting material outside the normal beam line. The spurious target material is fixed (since only the target holder moves), and its thickness is probably somewhat greater than

the thickness of the true targets. Specifically, we have in mind the two 0.020-in.-thick aluminum annular windows of the ion chamber to which the 0.0015-in.-thick Mylar windows are epoxied, as well as the epoxy itself, and possibly the larger flanges and beam pipe. Letting f be the fraction of the beam outside of the normal beam line and assuming a spurious thickness here of t_s in addition to whatever target is in the beam,[39] we obtain experimental rates of

$$R_0=(1-f)[t_0T+\tfrac{1}{2}t_0^2P]+f[(t_0+t_s)T+\tfrac{1}{2}(t_0+t_s)^2P]$$
$$=t_0T+ft_sT+\tfrac{1}{2}t_0^2P+\tfrac{1}{2}f(t_s^2+2t_0t_s)P, \quad \text{(B3a)}$$

$$R_1=(t_0+t_1)T+ft_sT+\tfrac{1}{2}(t_0+t_1)^2P$$
$$+\tfrac{1}{2}f(t_s^2+2t_0t_s+2t_st_1)P, \quad \text{(B3b)}$$

$$R_2=(t_0+t_2)T+ft_sT+\tfrac{1}{2}(t_0+t_2)^2P$$
$$+\tfrac{1}{2}f(t_s^2+2t_0t_s+2t_st_1)P. \quad \text{(B3c)}$$

The new expression for (R_1-R_0) agrees rigorously with the previous one except for the term

$$\Delta(R_1-R_0)/(R_1-R_0)$$
$$=(ft_s)t_1P/[t_1T+\tfrac{1}{2}(2t_1t_0+t_1^2)P]. \quad \text{(B4a)}$$

The factor ft_s also appears as a constant additive term in the target-thickness measurements made during the data run using the bremsstrahlung tail of the primary beam. The agreement of the weight/area value of t_0 with the value given by the bremsstrahlung data indicates that ft_s/t_0 is less than 1%

$$ft_s<0.01\times t_0<1\times10^{-5}X_0. \quad \text{(B4b)}$$

Substituting $t_0\sim t_1\sim10^{-3}X_0$, and assuming $2T/P\sim0.003$-X_0 at 500 MeV, we find from Eq. (B4a)

$$\Delta(R_1-R_0)/(R_1-R_0)\sim(ft_s)t_1P/3t_1^2P<1/300. \quad \text{(B4c)}$$

Similarly, we have

$$\Delta(R_2-R_0)/(R_2-R_0)\sim(ft_s)t_2P/\tfrac{1}{2}t_2^2<1/1000. \quad \text{(B4d)}$$

The effect contributes positively to both T and P.

From the experimental result, $B/R_0\sim0.4$, we can calculate the spurious target thickness as well as the fraction of the beam involved. The ratio of the background to the true empty-target rate is given by

$$B/(R_0-B)\sim f[t_sT+\tfrac{1}{2}(t_s^2+2t_0t_s)P]/[t_0T+\tfrac{1}{2}t_0^2P]$$
$$\sim(ft_s)[T+\tfrac{1}{2}(t_s+2t_0)P]/[t_0T+\tfrac{1}{2}t_0^2P]$$
$$<5t_s.$$
$$t_s>\tfrac{1}{5}(0.4/0.6),$$
$$t_s>0.13X_0. \quad \text{(B4e)}$$
$$f<1\times10^{-5}X_0/0.13X_0$$
$$<8\times10^{-5}. \quad \text{(B4f)}$$

In summary, the background in this model results from less than 10^{-4} of the primary beam being outside of the 5-cm-diam clear region. This "beam halo" strikes a spurious target of greater than $0.13X_0$ effective thickness which may consist of the annular aluminum windows of the ion chamber as well as of the flanges and beam pipe. These numbers seem to us quite plausible, and we consider this to be the most probable source for the background observed. More importantly, this source, like the others considered, is subtractable in the sense of Eqs. (B2a)–(B2c); any background which results from a fraction of the beam f hitting a spurious additional target t_s must contribute less than 0.3% to the rates for either (R_1-R_0) or (R_2-R_0).

[39] The background is obviously subtractable if the true targets do not add to the spurious thickness outside the normal beam line.